CONTROL OF PHOTOVOLTAIC SYSTEM AND ELECTRIC VEHICLE CHARGING IN HYBRID MODE OPERATION

A DISSERTATION

SUBMITTED IN PARTIAL FULFILLMENT OF THE REQUIREMENTS FOR THE AWARD OF THE DEGREE

OF

MASTER OF TECHNOLOGY

IN

POWER SYSTEM

(2020-2022)

Submitted by:

MAMTA GUPTA

(2K20/PSY/10)

Under the supervision of:

PROF. MUKHTIAR SINGH

DEPARTMENT OF ELECTRICAL ENGINEERING

DELHI TECHNOLGICAL UNIVERSITY

(Formerly Delhi College of Engineering)

Bawana Road, Delhi-110042

JUNE, 2022

ELECTRICAL ENGINEERING DEPARTMENT

DELHI TECHNOLOGICAL UNIVERSITY

(Formerly Delhi College of Engineering)

Bawana Road, Delhi-110042

CANDIDATE'S DECLARATION

I, **MAMTA GUPTA**, Roll No. – 2K20/PSY/10 student of M.Tech (Power System), hereby declare that the project Dissertation titled "**CONTROL OF PHOTOVOLTAIC SYSTEM AND ELECTRIC VEHICLE CHARGING IN HYBRID MODE OPERATION**" which is submitted by me to the Department of Electrical Engineering, Delhi Technological University, Delhi in partial fulfilment of the requirement for the award of the degree of Master of Technology, is original and not copied from any source without proper citation. This work has not previously formed the basis for the award of any Degree, Diploma Associateship, Fellowship or other similar title or recognition.

Place: Delhi

Date**:**

MAMTA GUPTA

Roll No. 2K20/PSY/10

M.Tech (Power System)

Delhi Technological University

ELECTRICAL ENGINEERING DEPARTMENT

DELHI TECHNOLOGICAL UNIVERSITY

(Formerly Delhi College of Engineering)

Bawana Road, Delhi-110042

CERTIFICATE

I hereby certify that the Project Dissertation titled "**CONTROL OF PHOTOVOLTAIC SYSTEM AND ELECTRIC VEHICLE CHARGING IN HYBRID MODE OPERATION**" which is submitted by **MAMTA GUPTA**, whose Roll No. is 2K20/PSY/10, Electrical Engineering Department, Delhi Technological University, Delhi in partial fulfilment of the requirement for the award of the degree of Master of Technology, is a record of the project work carried out by the students under my supervision. To the best of my knowledge this work has not been submitted in part or full for any Degree or Diploma to this University or elsewhere.

Place: Delhi

Date**:**

PROF. MUKHTIAR SINGH

(SUPERVISOR)

Department of Electrical Engineering

Delhi Technological University, Delhi

Shahbad Daulatpur, Delhi-110042

India

ABSTRACT

In the last couple of decades, the growing concern in the energy sector is mainly due to continuous depletion of fossil fuels and emission of carbon di oxide which leads to green-house effect. For sustainable management of conventional resources and for minimizing hazardous environmental condition, further research and development is required, in the field of alternate energy sources. Solar powered energy is one of the most widely used non-conventional energy, as it is abundant, inexhaustible, free and clean.

One of the major sectors using fossil fuel and natural gas is the transportation sector, hence battery electric vehicle was developed as an alternative to Internal Combustion (IC) engines, for reducing emission of CO_2 and to limit the use of fossil fuel. No emission EVs are majorly charged using electricity grid, where the major concentration of fuel mix comes from conventional sources, hence PV powered EV charging is a sustainable option for long term. However, energy supplied by PV system being dependent on various environmental factors such as temperature, irradiance etc. is not fixed. Hence there is a need of integration of PV with electricity grid and other multi-functional operating sources for reliable operation of EV charging.

In this work detailed simulation study of hybrid operation of photovoltaic (PV) and electric vehicle (EV) charging system is done. The renewable integrated EV charging infrastructure can be employed in diverse load power requirement scenarios. The overall system uses various converters at each stage, boost converter for harnessing solar PV power, a bi-directional buck-boost converter for EV charging, and a voltage source converter (VSC) with LCL filter for integrating overall system with the grid. The associated controllers for EV charging/discharging and for controlling various power flow mode consist of a controller at bi-directional DC to DC and at AC to DC stage. The proposed system contributes towards maximizing energy output from PV system, uninterrupted EV charging, reducing load demand

on grid for enhancing grid performance and using EV as an energy storage system as and when required. Extensive simulation for various power flow modes have been performed to verify the aforementioned claims.

Since large scale integration of renewable on main grid can lead to high voltage fluctuation. Hence BESS and on/off grid type inverters can act as a backup to manage black starting, islanding and any fault situation. To avoid system complexity a small sub model is also presented showing power flow management to load during on-grid to off-grid operation.

The overall design and simulation work is executed in MATLAB/Simulink software and results are confirmed for various input conditions.

ACKNOWLEDGEMENT

I would like to thank to all the people who have helped and inspired me during my dissertation work throughout these years.

I would like to express my sincere gratitude to my guide **Prof. Mukhtiar Singh**, Department of Electrical Engineering, Delhi Technological University, New Delhi, for his continuous support which helped me to complete this project work. His patience, motivation and immense knowledge has been a guiding light for me. His readiness for consultation at all times, and assistance have been invaluable which motivated and guided me throughout the period of work.

I would like to thank my seniors **Dr. Aakash Kumar Seth, Ms. Nimmi, Mr. Gaurav Kumar Yadav** for their guidance and continuous support in completion of this project work.

I wish to express my love and gratitude to my beloved parents, siblings and friends for their continuous support, encouragement and endless love. Above all, I would like to thank to the Almighty for blessing and guiding me, during all the ups and down throughout my life.

MAMTA GUPTA

Roll No. 2K20/PSY/10

CONTENTS

LIST OF FIGURES

LIST OF TABLE

LIST OF SYMBOL AND ABBREVIATION

Symbol and Abbreviation	Description
P_{pv}	PV Power
V_{oc}	Open circuit voltage of PV array
V_{dc}	DC link voltage
V_{bat}	Battery voltage
I_{bat}	Battery current
P_{bat}	Battery power
SOC	State of charge
V_{grid}	Grid voltage
f_{sw}	Grid frequency
L_i, L_g	Filter inductor
C_f	Filter capacitor
I_q	Quadrature axis current
I_d	Direct axis current
EV	Electric Vehicle
PVs	Photo Voltaic system
MPPT	Maximum power point tracking
CS	Charging station
V2G	vehicle to grid
G2V	Grid to vehicle
DPC	Direct power control
PI	Proportional integral
PWM	Pulse width modulation
SRFT	Synchronous reference frame theory
PLL	Phase locked loop
PCC	Point of common coupling

CHAPTER 1

INTRODUCTION

1.1 GENERAL

Energy is crucial for evolution of human civilisation. Energy is essential for our world's economic and social development. Energy is a universal currency and its consumption is used as a marker to distinguish between developed and developing countries. In comparison to others, a country's energy use distinguishes its measure of growth and development. In the last couple of decades, the growing concern in the energy sector is mainly due to continuous depletion of fossil fuels and emission of carbon di oxide which leads to greenhouse effect.

Conventional energy sources such as coal, crude oil, and natural gas are still widely used to generate power, but renewable resource use has improved the implementation since the 1970s. [1] For sustainable management of conventional resources and for minimizing hazardous environmental condition, in the field of alternate energy sources further research and development is required. Renewable energy sources are part of India's ambition to offer clean, affordable energy to everyone while simultaneously achieving social fairness and addressing environmental concerns. India has already begun the move to a cleaner environment, energy independence, and a stronger financial system by tapping these energy sources. India has ensured that the best methods for accelerating deployment, stimulating new firms, and accomplishing climate change mitigation targets are used. India is well on its way to meeting its target, with over 78 GW of installed renewable generating generation and 65 GW in various phases of development. Solar power capacity has increased by nearly 11 times since 2014, while wind power capacity has increased by 1.7 times. India now possesses the world's fifth-largest installed renewable energy capacity. This goal, however, is just the start, not the end. [2]

According to a study done by the European Commission by the year 2050 renewable energy source would establish its sovereignty over world’s energy supply system having percentage share of different forms as shown in Fig. 1.1.

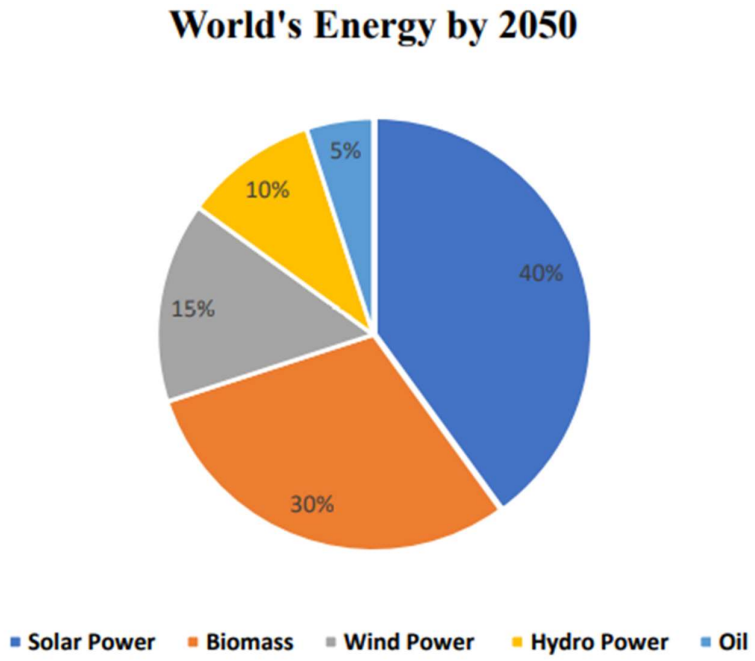

Figure 1.1: World energy consumption by the year 2050

Solar energy, wind energy, hydro energy, tidal energy, geothermal energy, and other renewable energy sources are available across worldwide. Since the sun is an unlimited source of energy, it may be used indefinitely for increasing energy demands, lowering electricity consumption rates, a wide range of uses, and minimal maintenance costs [3].

Photovoltaic systems are being used to extract solar energy in the majority of solar-based projects. This photovoltaic (PV) system is based on the idea that when solar irradiation strikes the surface, an ionisation process occurs, converting solar energy into electrical energy [4]. There has been continues research and development going on in the field of photovoltaics to lower their size, cost, and improve their conversion efficiency. Solar powered energy is one of the most widely used non-conventional energy, as it is abundant, inexhaustible, free and clean [5].

1.2: Photovoltaic systems

PV power generation systems are classified into two categories: grid-connected PV solar systems and stand-alone PV solar systems. As illustrated in Fig. 1.2 PV systems are classified according to their operation and application.

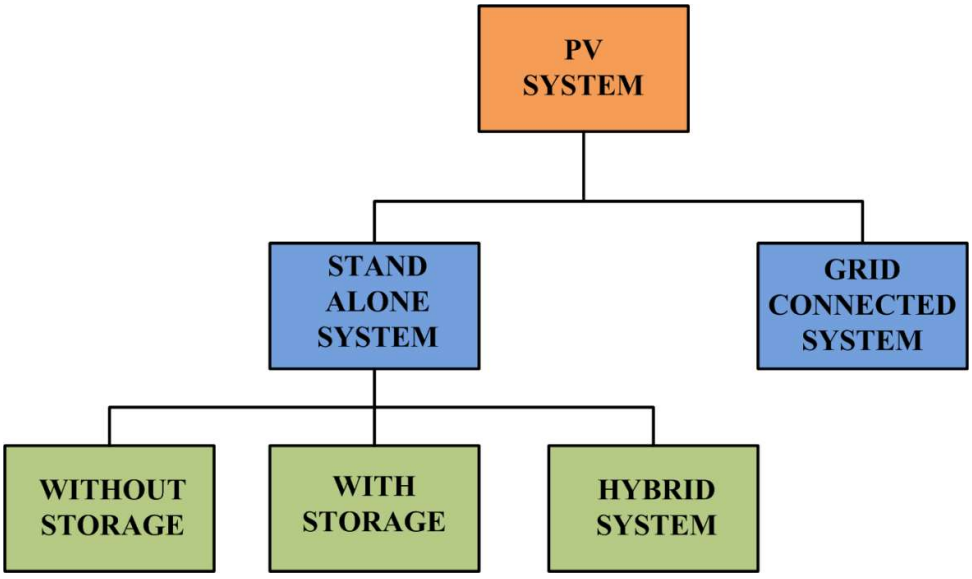

Figure 1.2: Classification of Photovoltaic systems

A stand-alone photovoltaic solar system is the best option in the places like rural area or area where supplying power through grid is difficult. According to the need of the application, the stand-alone system can be employed with or without power storage devices, as well as with a hybrid system [6]. However, using a stand-alone system for general-purpose applications during the night and in unfavourable weather conditions is challenging without power storage capacity.

In the grid connected PV system [7], the energy supply from the solar panels can be supplemented by AC power from the grid. Solar panels, on the other hand, can provide enough electricity to cover any grid loss.

1.3: Grid interconnected solar PV system, benefits and challenges

Grid connected PV system uses hysteresis current control (HCC), voltage source inverter (VSI) for the integration of the solar PV system to the grid. The DC-link capacitor can be linked directly to the grid-tied photovoltaic system, or it can be integrated to the DC-link capacitor via a boost converter before being fed to the inverter for power conversion and then electricity transferred to the three phase grid. MPPT control techniques are incorporated to converters to harness the peak power from a PV system and transfer it to the grid while also mitigating power quality issues. These approaches could also be used to measure the performance of a Photovoltaic system. The VSI delivers

solar power to the main grid and can compensate for reactive power and eliminate harmonics at common coupling point (PCC) [8].

Traditional control algorithm such as perturb and observe algorithm (P&O), incremental conductance methodology (INC), fractional current control, fractional voltage control, as well as intelligent method such as artificial neural network (ANN), fuzzy logic control, and other AI techniques [9] are available to harness the point of maximum power.

The Three-Phase VSI transforms DC into AC power and transmits it into the main grid. Various control strategies are employed to maintain the grid voltage and frequency at the common coupling point for grid synchronisation. SRFT, instantaneous reactive power theory (IRPT), power balance theory, conductance based current algorithm, etc. are control methods are available for implementing the VSI [10].

The voltage source converter of PV integrated grid system is controlled through enclosed loops. The main motive is maintaining voltage and frequency of grid at PCC for synchronisation and to inject pure sinusoidal current into the grid. The inner current control loop is used to regulate current. To utilise simple PI controller it is necessary to obtain the synchronously spinning d-q frame, and the abc to d-q transformation changes the AC signal into decoupled signal. On continuous signals in dq reference frames, PI controllers are used to ensure the track for reference is adequate with implementation and easy design.

There are many benefits of grid connected PVS for example improvement in power system reliability by having generation diversity and reduction in peak power. Improvement in voltage profile, reduction of line losses, control of reactive power is better, security of critical loads can be enhanced, facility of ancillary services, reduction of greenhouse gas emission etc are some of the many advantages of grid connected PVS [11].

Additional technical challenge for utilities and customer-generators is issues related to power quality. Since devices and appliances are designed to receive power at or near defined voltage and frequency parameters, and variations may result into appliance failure or damage, hence power should be constantly supplied at a standard voltage and frequency. A PV inverter might introduce unwanted noise into the system.

Power quality standards include harmonics, power factor, DC injection, and voltage flicker, islanding in addition to simple voltage and frequency ranges. [12]

In the literature [13] - [15], various topologies of grid integrated PV systems have been discussed. An adjustable DC-link with two stage grid tied solar PV system is presented [16], and an elimination of one stage leads to single stage topology having their own benefits and drawbacks. Topologies are also dependent on certain other factors such as isolation, power level requirement and controlling strategy. In [17], the elimination of boost converter is presented, here DC bus directly connects solar PV array with VSC, allowing VSC to harness the peak power out of solar PV array.

1.4: Types of Electric Vehicle

One of the major sectors using fossil fuel and natural gas is the transportation sector, hence battery electric vehicle was developed as an alternative to Internal Combustion (IC) engines, for reducing emission of CO_2 and to limit the use of fossil fuel. EVs, are a green alternative because they do not require liquid fuel. They are highly responsive, have a lot of torque, and may save you money on petrol and maintenance compared to conventional gasoline-powered vehicles. [18]

EVs can be classified as:

- Battery Electric Vehicle - BEV refers to an electric vehicle with a single source of energy, such as a battery. The BEV is solely reliant on the energy stored in the battery pack. As a result, the range of a BEV is directly proportional to the battery pack's capacity. These vehicles can typically travel 100-250 kilometres on a single charger. Furthermore, BEVs are ecologically friendly and have a low operating cost. [19]
- Hybrid Electric Vehicle - These EVs have two energy sources: fuel cell and a battery pack. They consist of an internal combustion (IC) engine as well as an electric power train. In low-speed requirement when power required is low, the electrical energy source can be switched. These vehicles switch to an IC engine when high speed is required. [20]-[21]
- Plug-in Hybrid Electric Vehicle - PHEVs, like HEVs, have two powertrains (a gasoline engine and an electric motor), but the electric propulsion is the primary driving force. As a result, it necessitates a larger battery pack than a HEV. [22]

- Fuel cell electric Vehicle - FCEVs are electric vehicles that use a fuel cell to power the drivetrain. The advantage of such a vehicle is that the power generated by fuel cells produces no carbon, and the time it takes to recharge it is comparable to that of a conventional vehicle. However, due to limitations in FCEVs such as high fuel cell costs, hydrogen storage, and fuel cell life cycle, these cars are not widely used. [23]

1.5: Electric Vehicle charging levels

Inductive and conductive charging techniques are also possible. Inductive power transmission systems transfer energy without requiring a physical connection. It uses electromagnetic (EM) fields to wirelessly transfer electricity from transmitter to receiver. As a result, inductive charging has a lower efficiency and is more expensive than conductive charging. The conductive system, on the other hand, has actual electrical connection between the transmitter and the receiver. As a result, it is more efficient and less expensive than inductive systems. [24]- [26].

TABLE I EV charging levels

Specification	Level 1	Level 2	Level 3
Voltage	120V AC	240 V AC	200-800 V DC
Current(A)	15	40	60
Charging time	16-20 hrs	7 hrs	<1 hr

Low- and medium-range plug-in hybrids, as well as all-electric battery electric car users with low daily driving usage, can charge overnight at Level 1 charging level.

In Level 2 for charging house or public units, connection installation and a dedicated equipment may be required, while automobiles like the Tesla have the power electronics on board and merely require an outlet. A standard EV battery can be charged overnight using Level 2 devices.

Level 3 fast charging allows for charging much less than one hour. Similar to petrol stations, it can be built in highway rest stops and city refuelling sites. The power source could be direct DC.

Distribution transformer losses, voltage variations, harmonic distortion, peak demand, and thermal stress on the distribution system can all be exacerbated by level 2 and 3 charging. Reduced transformer life could have a substantial influence on transformer life, dependability, security efficiency, and the affordability of creating smart grids [27].

1.6: Battery Technology

Batteries are one of the most essential aspects that determines how well an electric vehicle performs. It is made up of electrochemical cells that are connected to the vehicle via external connections. The battery technology for EVs has progressed from the initial utilisation lead-acid batteries in the late 1800s to lithium-ion batteries in the 2010s, which are now found in the majority of EVs. A battery pack is a collection of different battery modules and cells. The battery pack that powers electric vehicles might have as few as 96 cells or as many as 2,976 cells. Primary and secondary are the two categories. Vehicle batteries are generally rechargeable secondary batteries in this case.

Because of their high energy density compared to their weight, lithium-ion and lithium polymer batteries are the most prevalent battery types in modern electric cars.

Challenges faced by EV battery is mainly due to:

- high cost
- life cycle of batteries
- charger's complications
- the lack of charging infrastructure
- range anxiety

Terminology related to battery technologies:

Battery Capacity: The battery capacity is defined as the amount of free charge generated by active material at the negative electrode and consumed by the positive electrode. To look at it another way, it's the total quantity of energy that can be stored in

a battery. It is expressed in ampere-hours (Ah) or watt-hours (Wh), with 1 Ah totalling 3600 coulombs (C)

Specific energy: It is calculated in watt-hours per kilogramme (Wh/Kg) and is gravimetric energy stored by the battery. The quantity of energy retained in relation to its weight is referred to as gravimetric energy.

Energy Density: It is calculated in watt-hours per litre (Wh/l) and is volumetric energy contained by the battery. The quantity of energy held in relation to its volume is referred to as volumetric energy.

State of Charge (SOC): The state of charge (SOC) is a percentage representation of the quantity of energy obtainable in a battery at any given time. SOC of fully charged battery is equivalent to 1 or 100% and fully discharged battery is 0 or 0%.

Type of Electric vehicle battery

Table II Batteries parameters comparison

Specification	Li-on	Ni-mH	Lead-acid
Energy density(Wh/l)	250-693 high	140-300 high	80-90 low
Charge-discharge cycles	300-500	180-2000	200-300
Merits	Highest energy density, no need of periodical discharge	High charging efficiency, environment friendly	Inexpensive, lowest self-discharge rate
Demerits	Expensive, moderate discharge rate	High discharge rate, high maintenance	Low energy density, environment unfriendly

1.9: Hybrid PV based EV charging system

Integration of EV with grid can also provide other ancillary services like regulation of voltage and frequency, peak shaving, can act as a virtual power plant and regulated spinning reserve with the smart grid [31]-[33]. Moreover, integration of EV on a huge scale and its unregulated connection into the power distribution system might poses various problem such as rising peak demand, harmonics, voltage imbalance and current distortion etc. [34]. Another issue is that no emission EVs are majorly charged using electricity grid, where the major concentration of fuel mix comes from conventional sources, hence PV powered EV charging is a sustainable option for long term [35]. Interconnection of solar PV system with EV charging in a coordinated manner mitigates impact of solar PV generation on power grid. However, PV integrated system with EV leads to system complexity and to avoid issues related to solar power fluctuation, there is a need of integration of PV with grid and other multifunctional operating sources for reliable operation of EV charging [35]-[36].

Despite charging stations (CSs) which has integration of renewable energy-power are the most feasible alternative for EV charging, their integration into an already installed charging system adds a power conversion stage, increasing the system's complexity and power loss. Furthermore, each conversion stage has its own controller, which must be linked with the present system. [37]-[39] As a result, designing an integrated infrastructure with multifunctional and multimode operating capacity is important, and so its imperative to design unified control and coordination between the numerous sources.[40]-[41]

Furthermore, many of the research only discusses the effectiveness of CS in either grid-connected or islanded mode. The solar PV panel, though, gets ineffective if the grid is unavailable, even though the sun (solar irradiance) is present, due to the single mode of operation in the grid-connected configuration. Additionally, in the islanded mode, the PV power is disrupted by the solar irradiance's unpredictability. As a result, a storage battery is needed to counteract the effects of changing solar irradiation. To avoid overcharging the battery storage, the maximum power point tracking must be disabled when the storage battery is completely charged.

In the microgrid inverter control, a reference voltage and frequency signals are required in the islanded mode. [42]

The microsource controllers (MCs) link the microsources and storage devices to the feeders in a microgrid, and the central controller (CC) coordinates the microsources [2]. The circuit breakers connect the microgrid to the medium voltage level electric grid at the point of common coupling (PCC). When a microgrid is connected to the power grid, the grid handles all operating voltage and frequency regulation; nevertheless, the microgrid continues to supply important loads at PCC, designed to act as a PQ bus. In islanded mode, a microgrid must run independently of the grid to regulate the microgrid's voltage and frequency, and so functions as a PV (power-voltage) bus. [43]- [46]

CHAPTER – 2

DESIGN OF PV-EV HYBRID SYSTEM

2.1: SOLAR PV CELL

The basic component of solar module is the solar cell. Silicon (Si) is a semi-conductor substance that is largely employed in cell production. To obtain either n type or p type material, it is doped with another material. Silicon is doped with electron-rich atoms (such as phosphorus, arsenic, and antimony) to make n-type material, whereas it is doped with electron-deficient atoms (boron, aluminium, and gallium) to produce p-type material. The formed two materials thus combine to form p-n junction. When solar irradiation comes into contact with the junction, it causes current to flow and thus power flow takes place.

When the two materials are combined, free holes from the p-type diffuse into the n-layer, leaving behind negatively charged ions. Free electrons diffuse into the n-layer, leaving behind positively charged ions. This, in turn, forms an electric field zone between the two layers, which stops the charge flow in its region. When sunlight strikes a cell, electron-hole pairs are formed, causing current to flow.

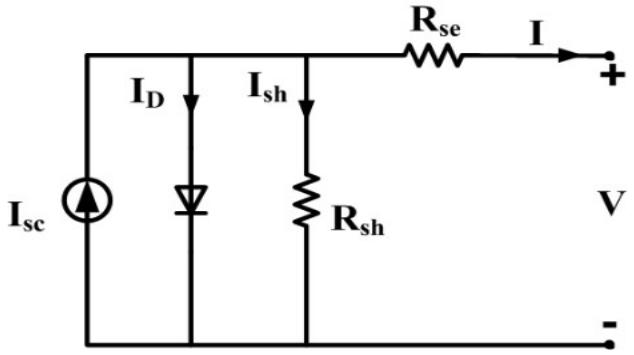

Figure 2.1: Electric equivalent PV cell model.

Fig. 2.1 shows equivalent electric circuit model of PV cell which is obtained after analysing its terminal characteristic, which is further utilized to design photovoltaic systems. Where,

R_{se}: R_{se} indicates the solar cell's series resistance. It appears due to current flow across the base-emitter junction of cell and metal-silicon wafer contact resistance.

R_{sh}: R_{sh} represents the shunt resistance of the cell. It exists because the p-n junction's properties aren't ideal, and there are impurities on the edges, causing a short circuit path around the junction. The series resistance would be 0 and the shunt resistance would be infinite in an ideal situation. R_{sh} and R_{se} are present due to nonlinearity in PV characteristic.

The terminal equation that governs the output voltage-current performance characteristic of PV cell is calculated as follows:

$$I = I_{sc-}I_D - I_{sh} \tag{2.1}$$

Where,

I is the output current of solar cell in Ampere, I_D is the current passing through the diode

Isc represents the photo electric current proportional to the total amount of perpendicular solar energy incident on solar cell surface,

According to Shockley equation diode current I_D is expressed as:

$$I_D = I_O(e^{\frac{V+IR_{se}}{nVt}} - 1) \tag{2.2}$$

I_o represents the reverse saturation current which is dependent on doping and temperature of p-n junction diode, q is the electron charge in columb, n denotes the diode ideality factor(assumed 1 for Germanium and 2 for Silicon), K is the is the Boltzmann's constant in Joule/Kelvin.

By performing nodal analysis, the shunt resistance current I_{sh} can be found out to be:

$$I_{sh} = \frac{V + I * R_{se}}{R_{sh}} \tag{2.3}$$

Therefore, now the output current can be expressed in the form as shown.

$$I = I_{sc} - I_O\left(e^{\frac{V+IR_{se}}{nVt}} - 1\right) - \frac{V+IR_{se}}{R_{sh}} \tag{2.4}$$

The above equation is an acausal equation but in practice diode is not ideal hence it has the junction capacitance which takes care of the causality problems.

A PV panel is made up of combination of many solar cells connected in series or parallel. This is done to make the panel's voltages and currents equal to the utility's parameter settings. Therefore, assuming C is the number of solar cells in series, Ns is the

number of series connected panels, and Np is the number of parallel connected panels, the array's characteristic equation becomes:

$$I = N_p I_{sc\_} I_D - I_{sh} \tag{2.5}$$

$$I_{sc} = \frac{Io + k(T_{op} - T_{ref})}{1000}\lambda \tag{2.6}$$

$$I_D = N_p I_O (e^{\frac{V+IR_{se}}{nN_s cVt}} - 1) \tag{2.7}$$

$$I_{sh} = \frac{N_p(V + I * R_{se})}{R_{sh}} \tag{2.8}$$

T_{OP} is the operating temperature of the solar cell in Kelvin, T_{REF} is the standard operating temperature of the cell in Kelvin λ is the solar irradiance in Watt/sq. meter

$$VT = \frac{T_{op} * K}{q} \tag{2.9}$$

Where VT represents the thermal voltage.

The characteristics of a practical solar panel can be represented using the equations above. They can be used to simulate and evaluate the panel in various settings in simulation environments (Simulink). This project makes use of the PV array module's built-in MATLAB/Simulink block, which is also centred on these equations.

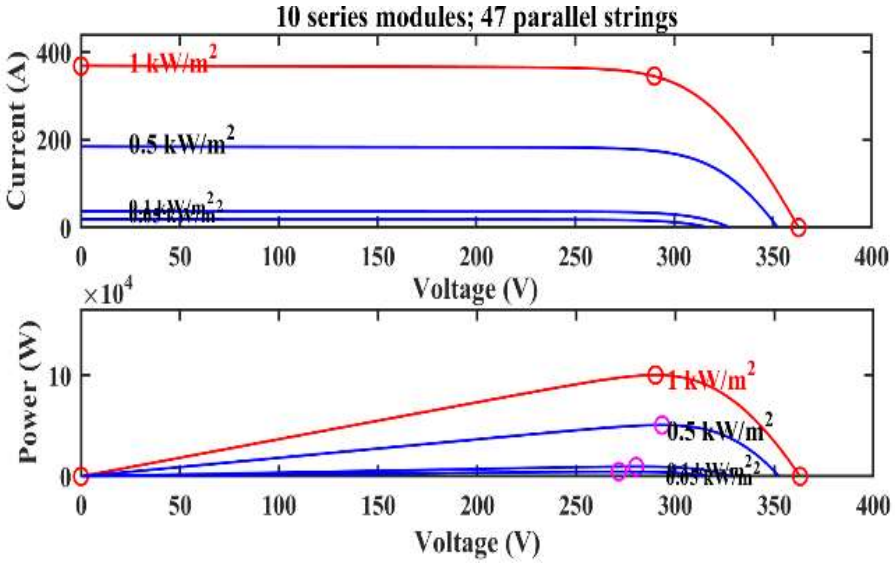

Figure 2.2: PV characteristic under different irradiance level

Under different irradiation levels, characteristic of I-V, P-V is drawn, which is depicted in Fig. 2.2 The nonlinearity in PV cell characteristic indicates that, the unique I-V characteristic results in output current which is constant over a wide voltage range until it extends to a point from where it begins to drop exponentially, giving rise to the concept of maximum power point which has to be tracked for exporting peak power out of solar array.

Changes in irradiance affect practically all parameters, including open circuit voltage, short circuit current, and efficiency. Since photo generated rate is proportional to irradiance, and short circuit current is proportional to photo generated current, this is the case. Irradiance, on the other hand, has a minor impact on open circuit voltage.

The open circuit voltage is much more affected by temperature changes than the short circuit current. Both of them are proportional to each other. The short circuit current, on the other hand, is unaffected by temperature changes.

Table III PV panel specification

Parameter	values
Open circuit voltage(V_{oc})	36.3 V
Short circuit current(I_{sc})	7.84 A
No. parallel string	47
No. of series string	10
Voltage at MPP (V_{mpp})	29 V
Current at MPP (I_{mpp})	7.35 A
Open circuit voltage of solar panel	363 V
Temperature coefficient of V_{oc}	−0.35%/ ℃
Temperature coefficient of I_{sc}	0.06%/ ℃

2.2: Design of Boost converter

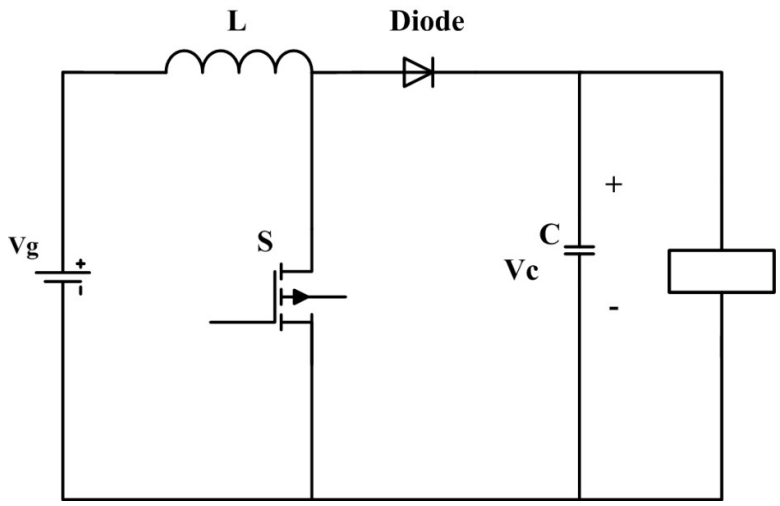

Figure 2.3: Boost converter

The boost converter is a DC-DC switching converter with a step-up capability. The low input voltage level can be boosted up to an useful high output voltage level using a boost converter, which works similarly to a reversed buck converter. Fig. 2.3. depicts the boost converter topology.

Current flows through the inductor (L) and energy is stored when the switch S1 is turned on by the PWM pulse. When the switch is switched off, the magnetic field energy stored in the inductor produces an induced voltage across the inductor, which adds to the input voltage. The input voltage and the voltage across the inductor are in series, causing the output capacitor (Cout) to be charged to a voltage greater than the input voltage.

When developing a conventional boost converter, the duty cycle is determined using equation based on the required output voltage.

$$D = 1 - \frac{V_o}{V_i} \tag{2.10}$$

Selection of inductor

The inductor value is chosen based on the estimated inductor ripple current at maximum input voltage, which is given by equation.

$$L = \frac{Vi(V_o - V_i)}{fs * \Delta I * V_o} \tag{2.11}$$

Where ΔIL is the estimated inductor ripple current. It should not exceed 5% of rated input current. Fs denote boost converter switching frequency. Here a switching frequency of 5 kHz is chosen.

Selection of capacitor

$$C = \frac{I_o(V_o - V_i)}{fs * \Delta I * V_o} \tag{2.12}$$

Where ΔV_o is desired output voltage ripple, for 1% voltage ripple corresponding to output voltage

2.3 Boost MPPT control

The main function of DC-DC boost converter is to rise the source side solar PV array voltage to load terminal by adjusting the duty cycle. This duty cycle, for maximum power is maintained by MPPT techniques.

Because I-V and P-V properties are influenced by solar irradiance and temperature, which change during the day, MPP varies as well. If the PV array is directly linked to the load, the operating point of PV is determined by the load impedance and environmental conditions, but not always, resulting in MPP operation, which underutilizes PV characteristics. we use the MPPT techniques with the DC-DC converter to get the most power out of the PV array. When the variable load is attached, the MPPT goal is to operate the PV at MPP regardless of changes in environmental conditions.

$$P_m = V_{mp} * I_{mp} \tag{2.13}$$

The MPPT technique is implemented in the PV solar system using the DC-DC converter (boost converter, buck converter, buck-boost converter etc) several control techniques are used to control the duty cycle of the DC-DC converter.

MPPT control algorithm are mentioned below

- Perturb and observe
- Incremental conductance
- Fractional open circuit voltage
- Fractional short circuit current
- Neural network
- Fuzzy logic control

Among several MPPT techniques, Perturbation and observation (P&O) method is most widely implemented because of the limited number of parameters required, simplicity in its structure and ease in calculation. The parameter required to track MPP is current and voltage of PV panel as input values, which implies the association between output power and terminal voltage. This method iteratively perturbs, observes and generates output power to track maximum power point. If at certain PV module operating $\frac{\Delta P}{\Delta V} > 0$ then the perturbation of PV module output voltage should be increased toward MPP, if PV module operating point $\frac{\Delta P}{\Delta V} < 0$ then the perturbation of PV module output voltage should be decreased toward MPP. If the status of certain point is $\frac{\Delta P}{\Delta V} = 0$ then that point is the point of maximum power. The MPPT flow chart is shown in Fig. 2.4.

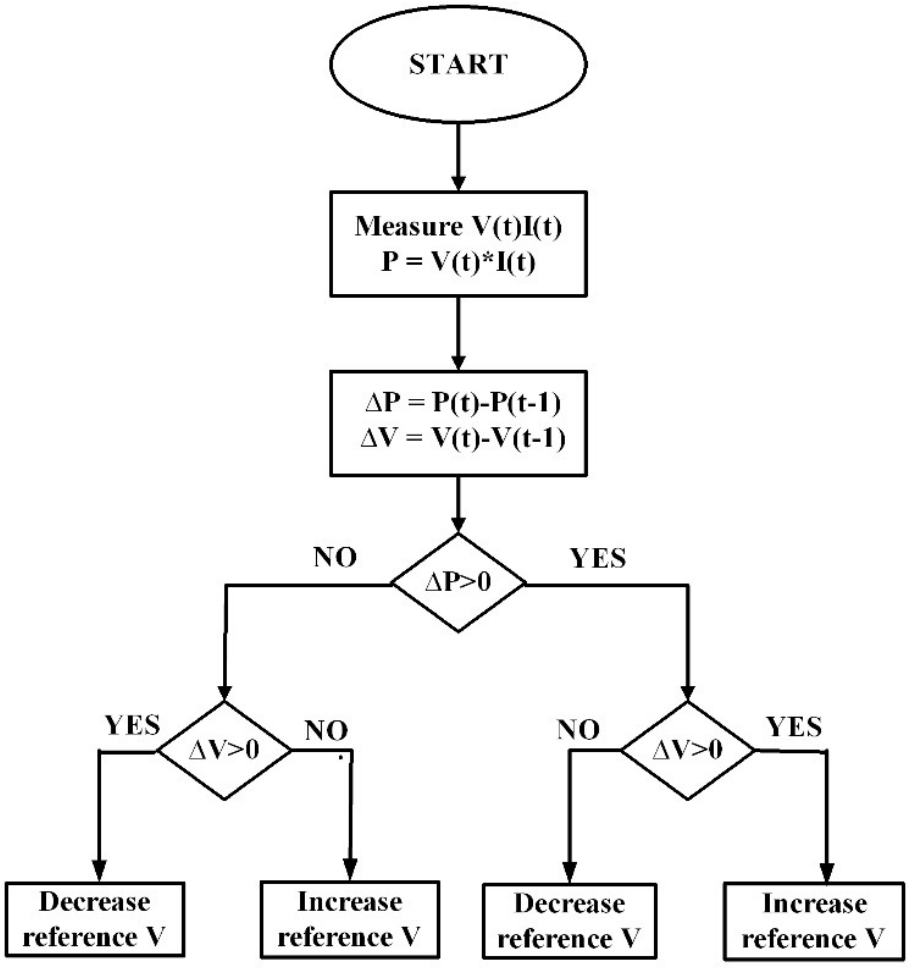

Figure 2.4: MPPT P&O flow chart

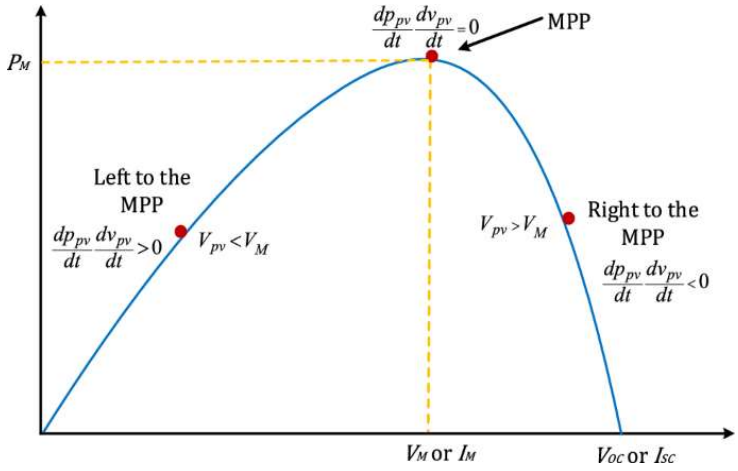

Figure 2.5: MPPT curve

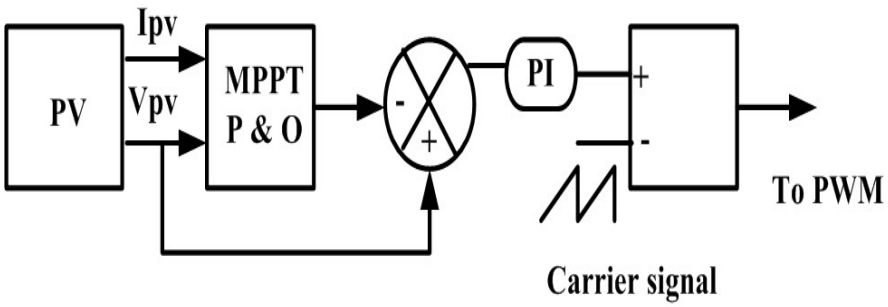

Figure 2.6: MPPT control

For boost converter control through MPPT, PV current and voltage is first sensed and passed through MPPT to generate V_{ref} which is the reference voltage for tracking MPP, error signal is generated by comparing V_{ref} with PV voltage, which is then passed to the PI controller , which will further generate signal having the required duty ratio, The output PWM signal is a result of comparing this generated signal with the carrier signal for the purpose of getting the required switching pulses for the boost converter as shown in Fig. 2.6.

2.4: Design of LCL filter

The converter implemented for PV to grid connection is bi-directional three phase AC to DC converter with sine pulse width modulation technique. The bidirectional power flow is important for this work as it allows power flow in both forward and reverse direction depending upon load requirement. For such an application appropriate control strategy of power switches of converter is required.

The PV inverter section of the overall system consist of PV panel and DC link capacitor on the DC input side and an LCL filter connected with grid at the output ac side. The voltage generated by PV panel has to ensure a dc link voltage higher than peak ac voltage at all the time. To improve the power quality supplied to local load and that injected to grid it is required to eliminate switching harmonics generated from PWM, for improving this quality filters are required. There are many filter topologies for example L filter, LC filter and LCL filter etc., among various filter topologies LCL filter is the most suitable for providing better attenuation and coupling capability.

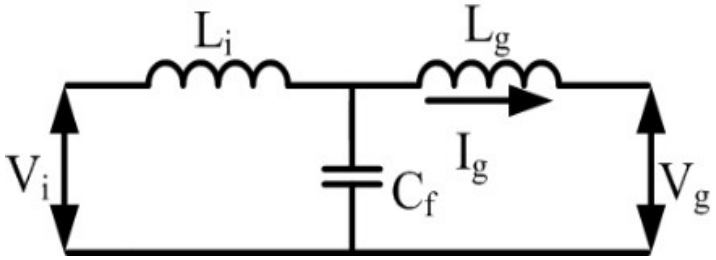

Figure 2.7: Single phase equivalent circuit of LCL filter

LCL filter has good ripple attenuation capability but can cause resonance related disturbance hence selection of filter components needs to be precise. For the design of filter, selecting filter components depends on several factors. Device constraint, cost and thermal consideration etc. influence switching frequency selection. The switching frequency of 10 kHz is chosen in this case.

For the design of the stated filter, there are normally some guidelines. To avoid a substantial voltage drop across the two inductors (i.e. $L_1 + L_2$), the total inductance of the two inductors (i.e. $L_i + L_g$) should be less than 10% of the system base impedance. The current ripple must not exceed 20% of the maximum rated current. When choosing a capacitance, it should not be too low or too high. A low number reduces the filter's effectiveness, whereas a large value absorbs a considerable quantity of reactive power. The inherent resonance frequency may fall within the range indicated by the equation. The sampling frequency is f_s, and the fundamental power frequency is f_g.

The inductance present over grid side L_g should be a fraction of the inverter side inductance L_i for excellent system stability. Finally, according to IEEE 519-1992, the THD of grid current shall not exceed 5%.

$$10fg<fs<0.5fs \tag{2.14}$$

Selection of switching frequency is based on device constraint, cost and thermal consideration. Here a switching frequency of 10 kHz is chosen. The fundamental and switching frequency both must be very well separated from resonant frequency for its selection.

The resonant frequency of LCL filter can be calculated as:

$$W_{res} = \sqrt{\frac{Li+Lg}{Li*Lg*Cf}} \tag{2.15}$$

The transfer function of LCL filter neglecting damping, all higher order harmonics condition, and by setting condition of $V_g = 0$ as shown in Fig. 2.7 is as follows:

$$\frac{Ig(s)}{Vi(s)} = \frac{1}{S^3 L_i L_g C_f + S(L_i + L_g)} \tag{2.16}$$

The capacitance value is determined based on reactive power requirement of capacitor. Due to this reactive power, overall output power factor is reduced causing large current to flow from IGBTs and L_i. The formula of capacitor C_f as shown in eq. 2.17 can be derived, with the limitation of reactive power requirement, keeping its value below 5% of inverter's rated output power.

$$C_f = \frac{0.05*S}{v^2*2*\pi*f} \tag{2.17}$$

For the minimization of ripple current flowing through switching IGBTs inverter side inductor is required. The total change in current during the overall cycle is expressed as:

$$\Delta i = \frac{V_{dc}}{F_{sw} * 2L_i}(1 - M_r \sin \omega_0 t) M_r sin w_0 t \tag{2.18}$$

Where F_{sw} is the switching frequency for the IGBT's, V_{dc} represents input DC-link voltage, ω_0 refers to the fundamental angular frequency and modulation index is represented by M_r.

The selection for the L1 inductor can be done in terms of the desired current ripple at the switching frequency

$$\mathrm{Li} = \frac{\mathrm{Vdc}}{8 * \Delta I L_{max} * f_{sw}} \tag{2.19}$$

In the eqn 2.20, the formula for computing the minimum total inductance necessary for the filter is described.

$$\mathrm{L} > \frac{\in \mathrm{Vdc}}{4 f_{sw} I_{rated}\, \zeta} \tag{2.20}$$

where ∈ represents the type of SPWM employed; value is 1 for Unipolar SPWM and 2 for Bipolar SPWM. Vdc is the ideal dc link capacitor voltage, Irated is the inverter's rated current, fsw is the PWM's switching frequency, and finally the symbol ζ is the maximum current ripple %. In this project, the value of has been set at 20% of the Irated.

As mentioned in the preceding section, the total inductance (i.e. L_i + L_g) should not exceed 10% of the rated current I_{rated}, as this causes a substantial voltage drop, which affects inverter operation. Both equations (2.21) and (2.22) should be satisfied by total inductance. The rated grid rms voltage is V_{rated}, the fundamental power frequency is f_o, and the rated apparent power of the system is S_{rated} in eqn. (2.21). The inductance value of grid side inductor is found using eqn. (2.23), where, γ is chosen to be 1.

$$L_i + L_g < 0.2 \frac{V^2{}_{rated}}{2\pi f_o S_{rated}} \tag{2.21}$$

$$L_i + L_g = L \tag{2.22}$$

$$L_i = \Upsilon L_g \tag{2.23}$$

Filter damping

Because of the presence of the LCL filter in the PWM control mechanism of the system depicted, there is a chance of resonance at the resonant frequency. Because of the LCL filter's inherent resonance problem. It is not possible to use a vector control mechanism directly. The resonance must be dampened using either a passive or active device/circuit. Connecting a small resistance in series with the filter capacitor is a simple but effective passive dampening approach. Adding a notch filter (with a cutoff frequency at the

resonance frequency) or employing capacitor current feedback are also active damping methods, however the latter adds a current sensor, which raises the cost.

The disadvantage of passive dampening technologies is that they reduce overall efficiency. Active damping systems, on the other hand, are susceptible to parameter changes and can become unstable. Furthermore, the controller bandwidth restricts the operation of active damping stability.

For passive damping a small resistance R_d is added in series with filter capacitor.

It is given by the following equation

$$R_d > \frac{1}{3 * w_{res} * C_f} \tag{2.24}$$

2.5: Minimum DC link voltage and size of DC link capacitor

A minimum dclink voltage is needed for proper rectifier operation in to get undistorted current waveforms. The rectifier's six diodes should be polarised negatively at all ac voltage supply values in order to have full control. We need a dclink voltage that is higher than the peak dc voltage delivered by the diodes alone to keep the diodes blocked.

Theoretically for diode rectifier, the maximum dc output voltage is the peak value of line-to-line RMS voltage.

$$V_{DCmin} > \sqrt{2}\, V_{LL}(\text{rms}) = \sqrt{2}.\sqrt{3}\, V_{LN}(rms) \tag{2.25}$$

It will be better to choose a DC-link voltage about 15-20% more than $\sqrt{2}V_{LL}$. This is a correct definition; however, it does not apply in every circumstance. The PWM approach determines the DC link voltage. Here we use a sinusoidal PWM in this scenario. The maximum reference voltage in this scenario is Vdc/2.

Here minimum DC link voltage will be given by equation

$$V_{LN}(peak) = V_{DC}/2 \tag{2.26}$$

$$\frac{V_{LL}(rms)}{\sqrt{3}}\sqrt{2} = V_{DC}/2 \tag{2.27}$$

$$V_{DCmin} > 2V_{LN}(peak) = \frac{V_{LL}(rms)}{\sqrt{3}}2\sqrt{2} = 1.663V_{LL}(rms) \tag{2.28}$$

$$C_{dc} = \frac{S_{rated}}{4 * \pi * f * V_{dc*}V_{rmax}} \tag{2.26}$$

V_{rmax} is the maximum permissible ripple voltage

2.6: Battery charger configuration

DC bus links EV batteries to off board charger. DC-DC converter is the basic building block and act as an interface to above battery charger configuration. The converter configuration as shown in Fig. 2.8. consist of two IGBT switches which always operate in complimentary fashion.

It permits power to flow in both directions, resulting in two modes of operation: buck and boost. When PV is incapable of operating it provides V2G operation hence EV acts as an auxiliary power supply leading to different modes of operation. The equation governing the above two operations are as follows:

$$\text{Boost mode: } V_H = \frac{V_L}{1-D} \tag{2.27}$$

$$\text{Buck mode: } V_H = \frac{V_L}{D} \tag{2.28}$$

V_H and V_L denotes voltages on high voltage and low voltage ends.

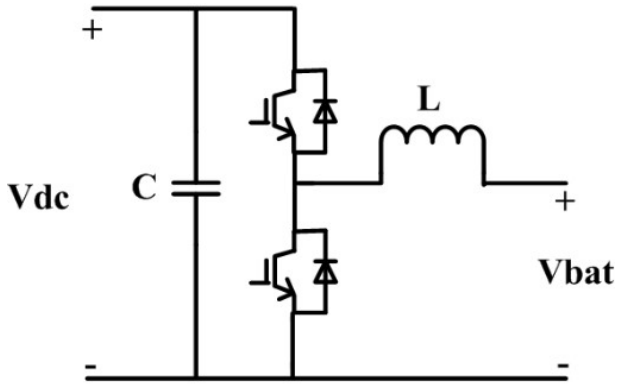

Figure 2.8: Buck boost converter

2.7: Modelling of Three phase AC-DC converter

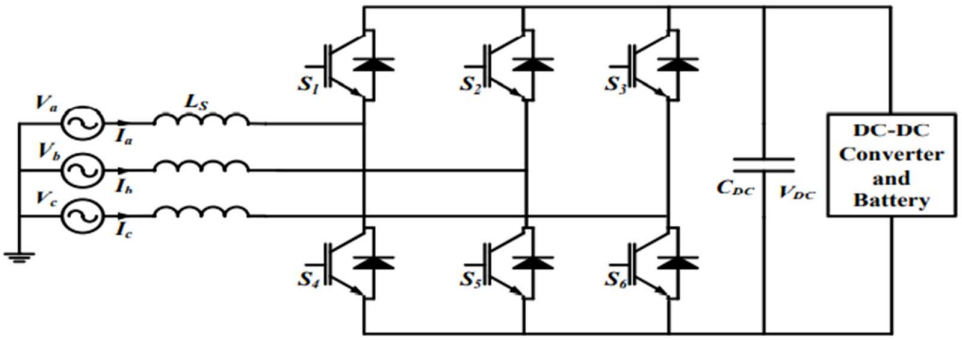

Figure 2.9: First stage of AC-DC converter

The configuration of three-phase AC-DC converter is shown in Fig. 3.4. The switching model shown in Fig. 2.9. is represented by three single pole double throw switches (Sa, Sb and Sc). The grid voltage is represented by V_{abc} where each phase voltage of charger is represented by V_{ga}, V_{gb} and V_{gc}, and line-to-line voltage is Vg_{ab}, Vg_{bc} and Vg_{ca}. The value of single pole double throw switch is 1 in case of upper switch on and 0 in case of lower switch on. The equations of three-phase voltages and currents are as follows

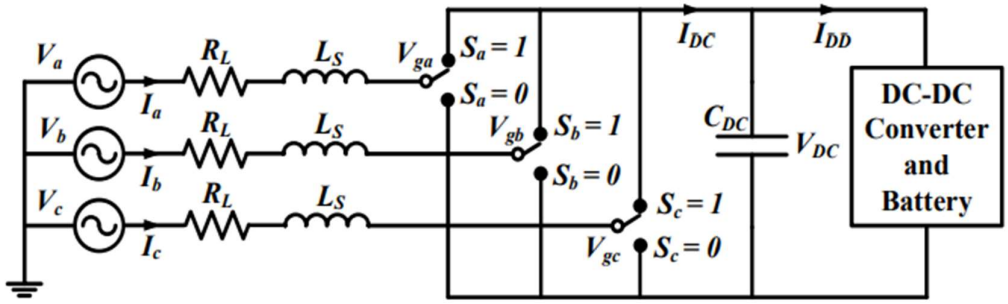

Figure 2.10: Switching model of three phase AC-DC converter.

$$V_{ga} = V_m \cos(wt) \tag{2.29}$$

$$V_{gb} = V_m \cos(wt - \tfrac{2\pi}{3}) \tag{2.30}$$

$$V_{gc} = V_m \cos(wt - \frac{4\pi}{3}) \tag{2.31}$$

$$I_a = I_m \cos(wt + \emptyset) \tag{2.32}$$

$$I_a = I_m \cos(wt + \emptyset - \tfrac{2\pi}{3}) \tag{2.33}$$

$$I_a = I_m \cos(wt + \emptyset - \frac{4\pi}{3}) \tag{2.34}$$

Since, neutral is not used here, we obtain

$$Ia + Ib + Ic = 0$$

From the switching model, the line-to-line voltage can be written as,

$$V_{gab} = (S_a - S_b).V_{DC} \tag{2.35}$$

$$V_{gbc} = (S_b - S_c).V_{DC} \tag{2.36}$$

$$V_{gbc} = (S_b - S_c).V_{DC} \tag{2.37}$$

Where, the switch (Sa, Sb and Sc) values are 1 in case of upper switch on and 0 in case of lower switch on.

$$V_{ga} = f_a.V_{DC} \tag{2.38}$$

$$V_{gb} = f_b.V_{DC} \tag{2.39}$$

$$V_{gc} = f_c.V_{DC} \tag{2.40}$$

Where,

$$f_a = S_a - \frac{1}{3}(S_a + S_b + S_c) \tag{2.41}$$

$$f_b = S_b - \frac{1}{3}(S_a + S_b + S_c) \tag{2.42}$$

$$f_{ac} = S_c - \frac{1}{3}(S_a + S_b + S_c) \tag{2.43}$$

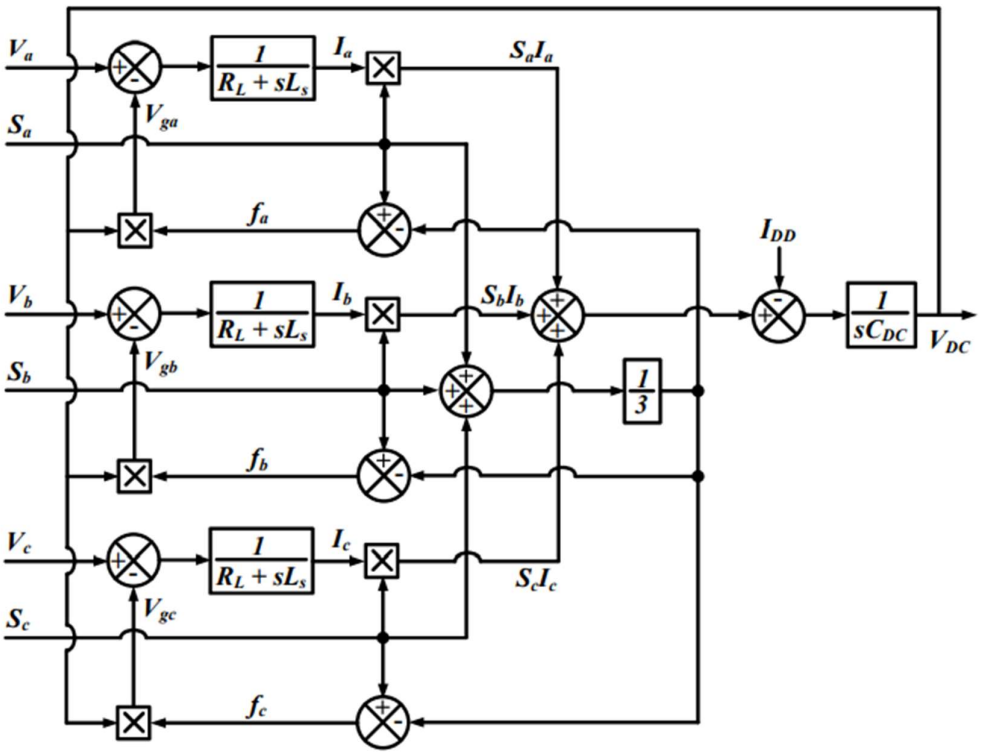

Figure 2.11: Block diagram of three phase AC-DC converter.

Apply KVL in each phase

$$V_a = R_L . I_a + L_s \frac{dI_a}{d_t} + V_{ga} \tag{2.44}$$

$$V_b = R_L . I_b + L_s \frac{dI_b}{d_t} + V_{gb} \tag{2.45}$$

$$V_{bc} = R_L . I_{abc} + L_s \frac{dI_{bac}}{d_t} + V_{gc} \tag{2.46}$$

By applying KCL at DC side,

$$C_{DC} \frac{dV_{DC}}{d_t} = S_a I_a + S_b I_b + ScIc - I_{DD} \tag{2.47}$$

2.8: DQ transform theory

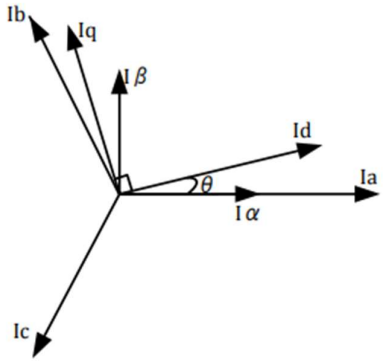

Figure 2.12: Transformation vector

The main problem when using proportional-integral (PI) controllers in order to control time varying signals such as sinusoidal currents and voltages is that the controller cannot reach zero steady state error. Therefore, to avoid this problem, synchronous reference frame can be used to represent the time varying signals as dc signals. The logic behind this is, a phasor which is rotating at an angular velocity ω will seem to be stationary relative to a reference phasor who is rotating at the same angular velocity ω in the same direction.

The Clarke transformation is expressed by the following equations:

$$I\alpha = 2/3\ (Ia) - 1/3\ (Ib + Ic) \tag{2.48}$$

$$I\beta = 1/\sqrt{3}\ (Ib - Ic) \tag{2.49}$$

where, I_a, I_b, and I_c are three-phase quantities Iα and Iβ are stationary orthogonal reference frame quantities The two-axis orthogonal stationary reference frame quantities are transformed into rotating reference frame quantities using Park transformation.

$$Id = I\alpha * \cos(\theta) + I\beta * \sin(\theta) \tag{2.50}$$

$$Iq = I\beta * \cos(\theta) - I\alpha * \sin(\theta) \tag{2.51}$$

where, Id, Iq are rotating reference frame quantities Iα, Iβ are orthogonal stationary reference frame quantities, θ is the rotation angle.

2.9: Phase locked loop

A phase-locked loop (PLL) is a system that produces an output signal with a fixed phase angle in relation to the input signal. One of the simplest ways to build PLL is to use a phase detector and a variable frequency oscillator in a negative feedback loop. The oscillator generates a periodic signal, which is compared to the input signal and outputs the phase difference between them, which is then minimised by the oscillator.

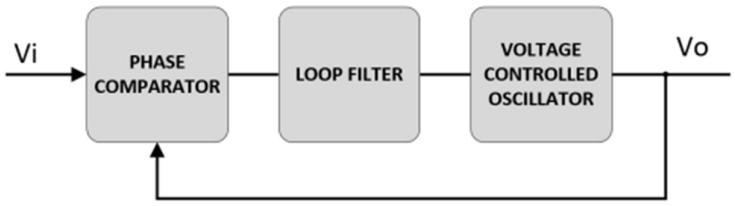

Figure 2.13: Simplest analog PLL

Maintaining phase lock also implies that the frequency is kept constant. As a result, the PLL can not only keep track of and synchronise with an input frequency, but it can also be used to generate frequencies that are multiples of the input frequency. Its features are used in clock synchronisation, high-frequency signal generation, and demodulation.

The PLL block in MATLAB is a closed loop system that uses a variable frequency oscillator to track the phase difference and frequency of the applied sinusoidal signal. The frequency is adjusted by the PID controller in the system to maintain zero phase difference. Fig. 2.14 shows the internal block diagram of the SRF-PLL.

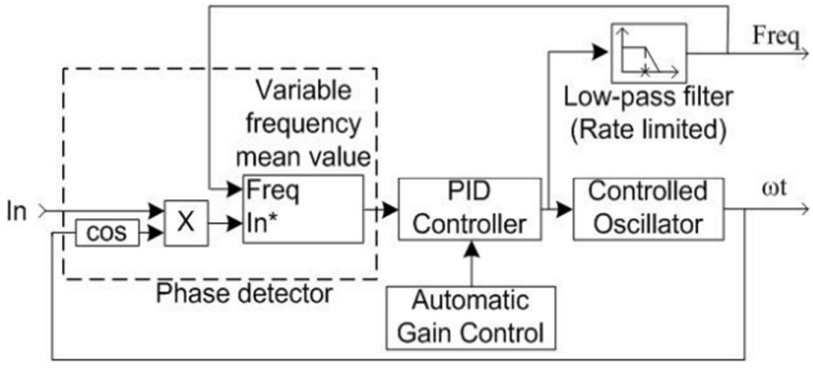

Figure 2.14: PLL subsystem block diagram

The oscillator's signal is superimposed on the input signal. The phase difference between the two signals is extracted by applying the DC component of this mixed signal to the variable frequency mean value. The phase difference is then tracked by a PID controller, which controls the oscillator to bring it to zero. The output of the PID (angular velocity) is passed via a low pass filter in the meantime.

CHAPTER 3

CONTROL DEVELOPMENT AND SIMULATION OF PHOTOVOLTAIC AND EV CHARGING HYBRID SYSTEM

3.1: SYSTEM DESCRIPTION

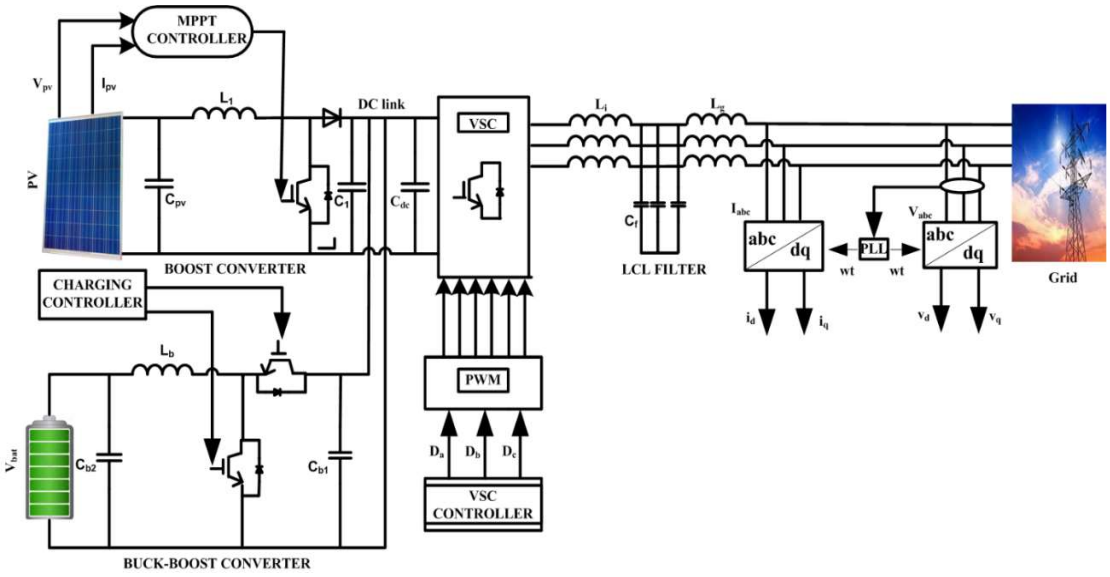

Figure 3.1: overall system configuration of grid tied PV-EV hybrid system

The complete system architecture is shown in Fig. 3.1. The system consists of PV source, grid and EV charging station.

In this work, boost converter harnesses peak power out of PV array, which is further interconnected with DC link of VSC for AC-DC conversion. The EV battery charger is interfaced at DC link with the help of DC-DC bi-directional buck-boost converter. The control algorithm prioritizes energy sources utilization based on solar power generation and EV charging requirement. Firstly, it utilizes solar power for EV charging and in case of less availability or over power generation remaining power is taken from or fed to grid respectively. EV can also be used as a form of storage system and during peak load time it can supply energy back to grid as and when required. During unavailability of solar power, EV and grid can act as an isolated system having both V2G and G2V mode.

The overall system configuration as shown in Fig. 3.1 is designed in MATLAB/Simulink software, where total seven power flow modes from mode 1 to mode 7, which has been discussed in Table II., is simulated to validate controller performance upon various input conditions and load power requirements.

3.2: VSC decoupled current control

The PI based controller design of VSC is depicted in the Fig. 3.2. The controller ensures DC-link voltage regulation. It is required for the reference value to be constant in its steady state for the necessary integral action of a PI based current controller to provide zero steady state error control, this can be achieved by applying Clarke's and park's transformation which is used to transform AC based current quantities into DC quantities and hence simple PI controller gives good result. The phase looked loop (PLL) is used to calculate ωt which maintains the synchronization between inverter current and grid voltage.

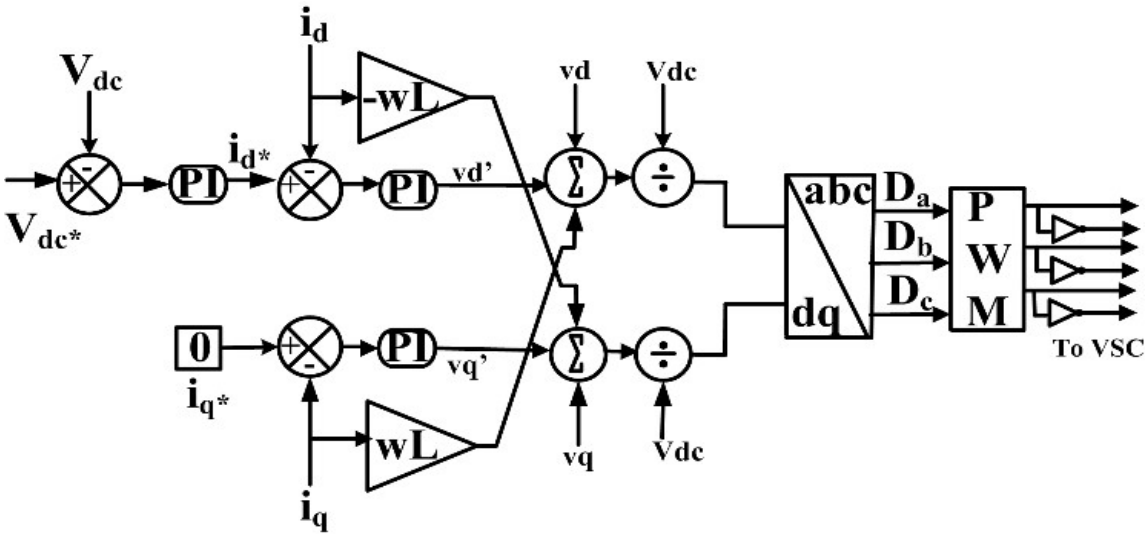

Figure 3.2: VSC decoupled current control

Since, PV based grid system is in combination with EV charging system, multimode controller combinations are required. Two control loops is used in this PWM based technique i.e. an outer slower voltage loop which is used to regulate DC link voltage and an inner fast current loop for controlling *dq* axis current (i_d and i_q). Since, the *d* and *q* axis values are interconnected, controlling the active and reactive flow of power into the grid requires the use of two PI controllers. The DC link voltage is regulated by the PI controller, by minimizing the difference between the reference and actual voltage values,

which further act as a reference for the *d* axis current (i_d^*). The line current vector must be aligned with the line voltage vector to achieve the condition of Unity Power Factor (UPF), hence the *q* axis current reference is set to zero ($i_q^* = 0$).

Design of Synchronous PI controller

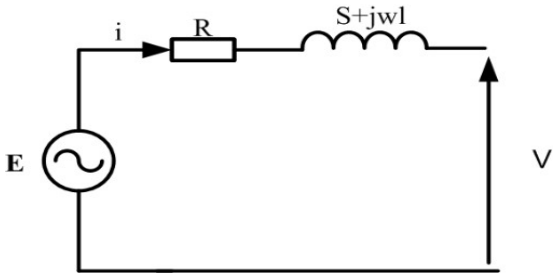

Figure 3.3: Synchronous coordinate schematic

Synchronous coordinates equation notation ($x = x_{dq} = x_q + jx_q$)

$$L\frac{di}{dt} = E - (R + jwl)i - V \tag{3.1}$$

$$(R+SL+jwL)i = E\text{-}V \Rightarrow i = \frac{E-V}{R+SL+jwl} \tag{3.2}$$

And the system transfer function G(s) is

$$G(s) = \frac{i}{V} = -\frac{1}{R+SL+jwL} \tag{3.3}$$

The important step of this controller design is to cancel cross coupling term initiated by *jwLi* (since multiplication by j maps d axis on q axis and vice versa). This is possible if we have an accurate prediction of L. For high performance and accuracy current tracking we need to cancel this cross-coupling.

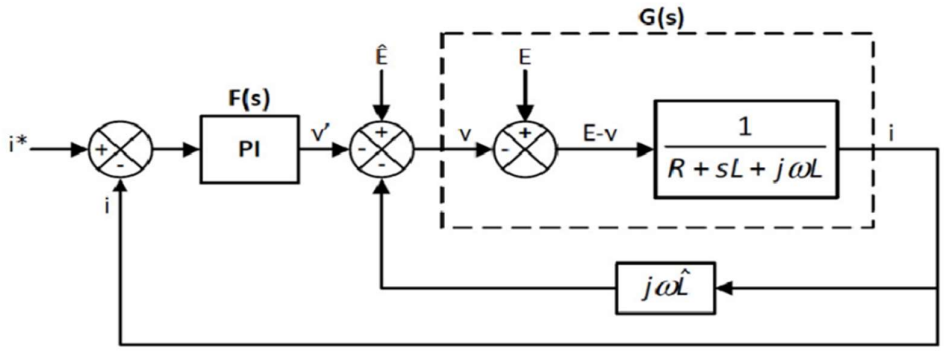

Figure 3.4: current control with inner decoupling loop

The expression for *dq* axis current is as follows:

$$\frac{di_d}{dt} = v_d - k_p v_d{}' - k_i i_d + wLi_q/L \tag{3.4}$$

$$\frac{di_q}{dt} = v_q - k_p v_q{}' - k_i i_q - wLi_d/L \tag{3.5}$$

Where L is the line inductance and w is the grid's angular frequency. In addition, ignoring inverter losses, the equation for active and reactive power is as follows:

$$P = \frac{3}{2} Re\{v^{dq}(i^{dq})^*\} = \frac{3}{2}(v_d i_d + v_q i_q) \tag{3.6}$$

$$Q = \frac{3}{2} Im\{v^{dq}(i^{dq})^*\} = \frac{3}{2}(v_q i_d - v_d i_q) \tag{3.7}$$

Since, $i_q^* = 0$ so voltage vector is aligned with d axis, we get:

$$P = \frac{3}{2}(v_d \times i_d) \tag{3.8}$$

$$Q = 0 \tag{3.9}$$

3.3: Battery charger control

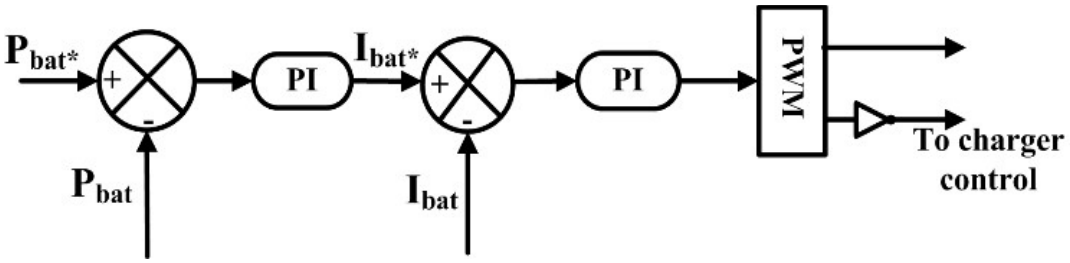

Figure 3.5: constant current control for EV battery

Fig. 3.5. depicts a PI controller-based constant current control that is used to control the charging and discharging of an electric vehicle battery. Depending on the direction of power flow, buck and boost mode is operated. Buck mode is used to charge the battery if the SOC is less than the threshold value, and boost mode is used to operate V2G if the SOC is larger than the threshold and based on required load power demand on grid.

The operation of a DC-DC bi-directional converter is determined by the amount of PV power generated, the state of charge (SOC) of the electric vehicle battery, and the load demand of the power grid. For proper operation of different modes, I_{bat} and P_{bat} are the two quantities which needs to be controlled by the controller, therefore two PI controllers are required. For outer loop battery actual power is compared with the reference power

to obtain the signal which will be further compared with battery current to generate switching pulses i.e. D. Based on the generated power reference and measured power, decision is made by the controller leading to operation of battery charging (buck) and battery discharging/V2G (boost) mode.

$$I_{bat}{}^{*} = (k_{p1} + \frac{k_{i1}}{s}) * (P_{bat}{}^{*} - P_{bat}) \quad (3.10)$$

$$D = (k_{p2} + \frac{k_{i2}}{s}) * (I_{bat}{}^{*} - I_{bat}) \quad (3.11)$$

3.4: System Parameters

Table IV System parameters

PARAMETER	SYMBOL	VALUES
PV Power	P_{pv}	100 kW
Open circuit voltage of PV array	V_{oc}	363 V
DC link voltage	V_{dc}	600 V
Boost inductor	L_1	1.45 mH
Boost capacitor	C_1	3227 µF
Battery voltage	V_{bat}	350 V
Battery SOC	*soc*	50 %
Buck boost inductor	L_b	4 mh
Buck boost capacitor	C_{b1}	100 µF
Grid voltage	V_{grid}	400 V
Grid frequency	f	50 Hz
Switching frequency	f_{sw}	10 kHz
Filter inductor	L_i, L_g	500 mH
Filter capacitor	C_f	100 µF

3.5: Simulation results of PV-EV hybrid system operation

To verify the performance claim of controllers, different modes of power flow as shown in Table II. are obtained depending on PV generated power, EV charging/discharging state, and grid power requirement. The PV system gives maximum power output of 100 kW and power varies according to irradiance condition 1000 $\frac{W}{m^2}$ − 500$\frac{W}{m^2}$ −1000 $\frac{W}{m^2}$ − 0 $\frac{W}{m^2}$ pertaining to different modes as shown in Fig. 3.7 (a). The DC-link voltage is maintained at its reference value of 600 V as inferred form Fig. 3.6.

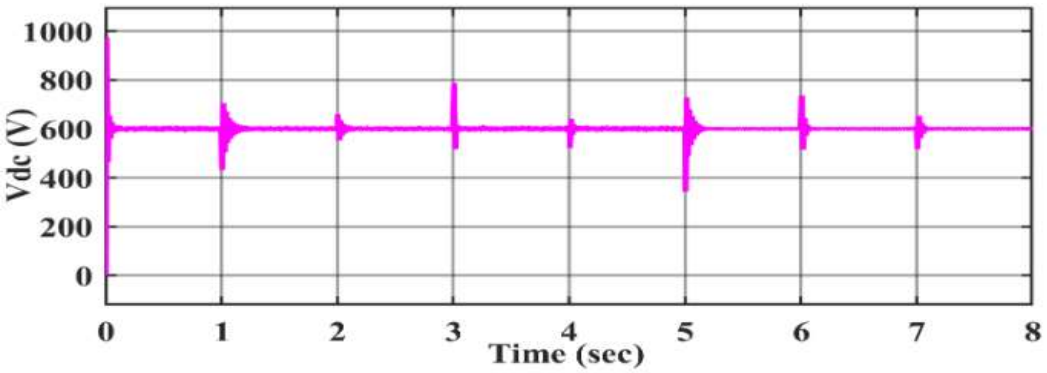

Figure 3.6 DC link voltage

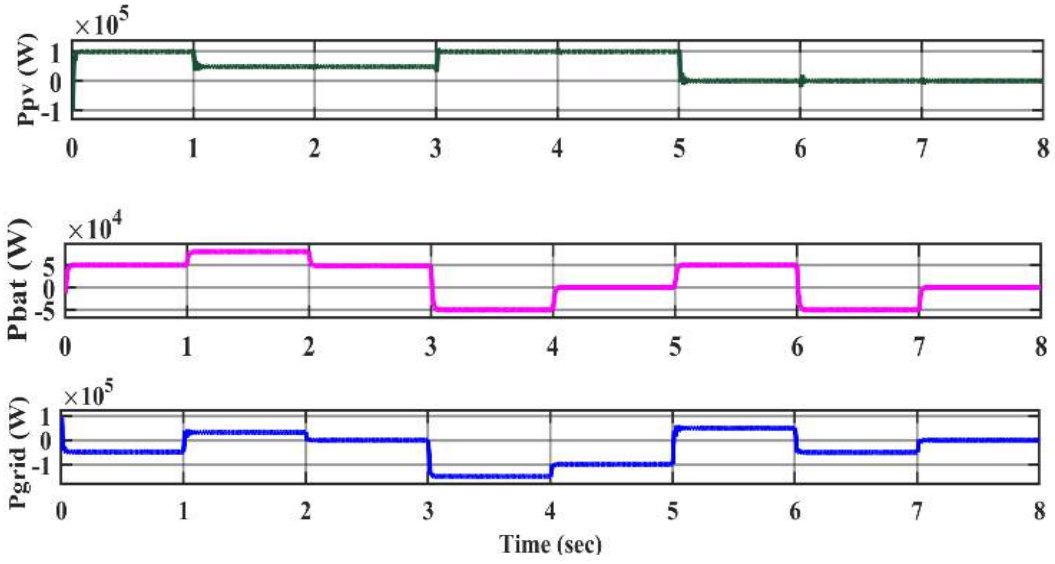

Figure 3.7: (a) Solar PV generated power (b) Battery power waveform during charging/discharge mode (c) Grid active power (P_{grid}).

The power for solar PV, battery and grid active power for different modes of operation are enumerated in Table V and shown in Fig. 3.6. During mode 1 generated PV power is used for charging of EV battery and power which is remaining is absorbed by the grid. Mode 2 shows EV charging through PV and grid both i.e. G2V mode is also shown here which will be required in case of increased EV charging demand and during the case in which PV is not sufficient enough to meet EV load demand. Mode 3 shows PV based EV charger which is isolated from grid. During the case of increase load demand on grid, mode 4 can be used where EV is acting as a storage system i.e. V2G operation and where both PV and EV are supplying power to meet the grid load demand. Mode 5 shows PV grid system isolated from EV. During mode 6 and mode 7, PV is isolated from EV and grid system, here G2V and V2G operations are shown respectively.

Table V Simulation results of PV-EV hybrid system operation

# MODE	IRRADIATION $\frac{W}{m^2}$	P_{PV} kW	P_{bat} kW	P_{grid} kW
1	1000	100	50	-50
2	500	48	80	32
3	500	48	48	0
4	1000	100	-50	-150
5	1000	100	0	-100
6	0	0	50	50
7	0	0	-50	-50

SOC, battery voltage (V_{bat}) and battery current (I_{bat}) are shown in Fig. 3.8 and 3.9 respectively. During mode 1 2 3 and 6 battery current is negative and battery power is positive which signifies battery charging state and in mode 4 and 7 battery current is positive and battery power is negative which signifies battery discharging state. Mode 5 is showing no action on EV. Battery voltage value is positive during all the stages. Battery SOC is increasing in mode 1 2 3 6 and decreasing in mode 4 and 7 signifying EV charging

and discharging respectively. SOC is increasing faster in mode 2 which means more power is supplied to the battery in this mode compared to other modes.

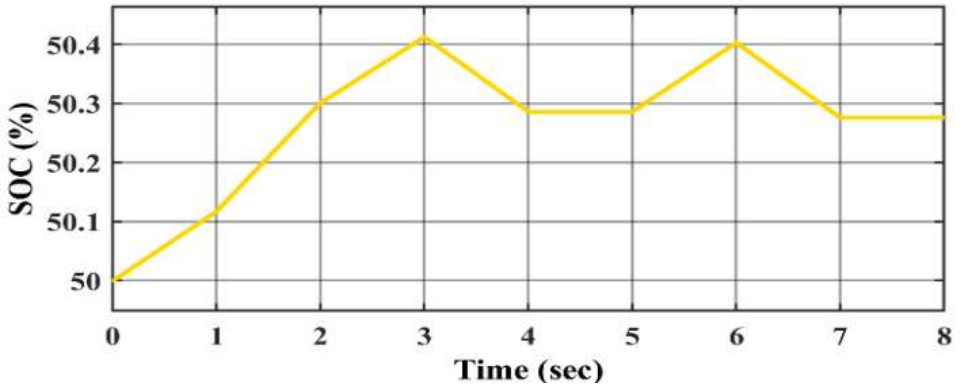

Fig. 3.8: SOC of battery

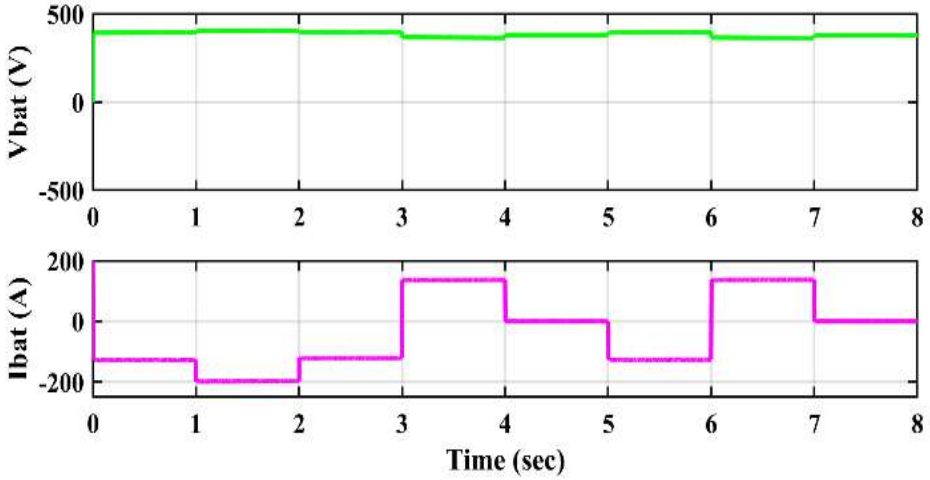

Figure 3.9: Simulation result of battery voltage V_{bat} and battery current I_{bat}.

Fig. 3.10 (a) and (b) shows instantaneous grid voltage and current. Mode 2 and 6 follows Fig. 3.10 (a) shows same phase between voltage and current and Fig. 3.6 (c). also signifies positive power for this modes i.e. power is supplied by the grid in this mode. Mode 1 4 5 7 follows Fig. 3.10 (b) and shows voltage and current in opposite phase and Fig. 3.6 (c). also showing negative power for all this modes i.e. power is absorbed by the grid in this case.

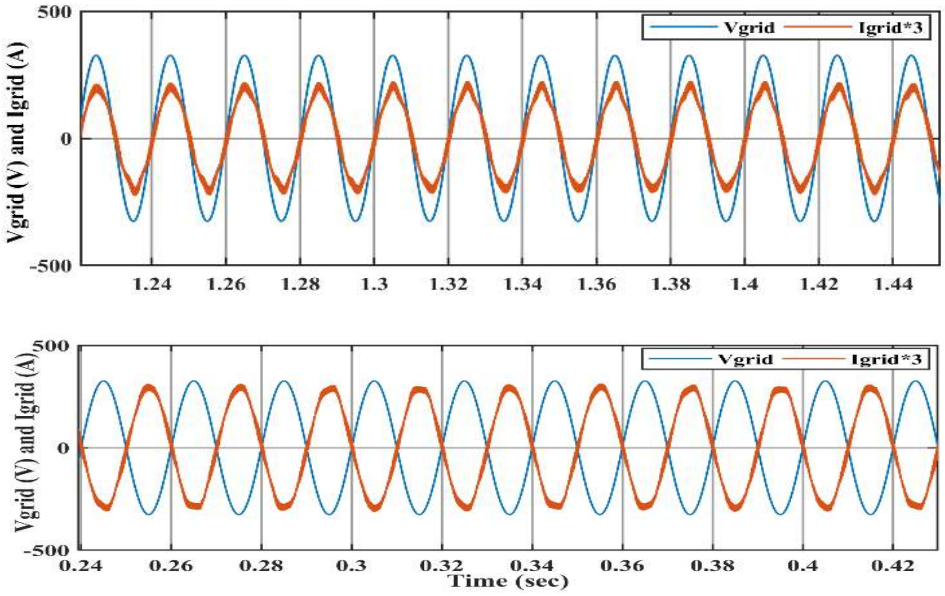

Figure 3.10: Simulation results of instantaneous grid voltage and current during (a) mode 2 and 6 is in same phase and (b) and during mode 1, 4, 5 and 7 in out of phase

CHAPTER 4

POWER FLOW MANAGEMENT DURING TRANSISTION THROUGH ON-GRID TO OFF-GRID MODE

4.1: Application of Battery Energy Storage System(BESS)

High power fluctuations are expected to become more regular in the coming years as the amount of renewable energy integrated into the main grid grows. As a result, there's a chance that blackouts will become more common in the future. (BESS) provide a backup supply for a small portion of the main grid and can manage black-starting and islanding situations. Severe power variations of the total power infeed in the electric power grid are projected to become widespread as a result of these integration of renewable technologies to main grid having variable infeed behaviour. The high variations between load and generation are caused by these power fluctuations. As a result, the necessity for increased flexibility in the power system to balance these differences is undeniable.

One method to increase flexibility is to use storage technology. As a result, long- and short-term storage technologies are likely to become more integrated into the power system. Battery Energy Storage Systems (BESS) are intended to meet a portion of the need for short-term storage for periods of minutes, hours, or days.

“Grid-connected mode" and "island mode" are the two operation modes of a system. In island mode, the operation of an off grid mode apart from the main grid is dependent on appropriate control algorithms.

The capacity to build the grid angle on their own distinguishes grid-forming converters from typical "grid-following" converters, whereas grid-following converters rely on grid angle estimation based on voltage measurements at their point of common coupling (PCC). The provision of an islanded micro grid by several grid-forming units necessitates the use of load-sharing strategies.

In a grid-connected system, islanding can be an intended separation from the main grid for maintenance purposes, or it can be an unscheduled disconnection Consequently

system may experience voltage fluctuations and sag swell mismatch of source output and load power and due to switch transient.

Because Li-Ion battery cells are becoming more affordable, this technology is expected to account for the majority of BESS in the future. In the context of value-stacking, islanding is viewed as an extra service that BESS can give to boost their profitability while also increasing supply reliability in the event of interconnected power grid disruptions by constructing local micro grids.

4.2: System description

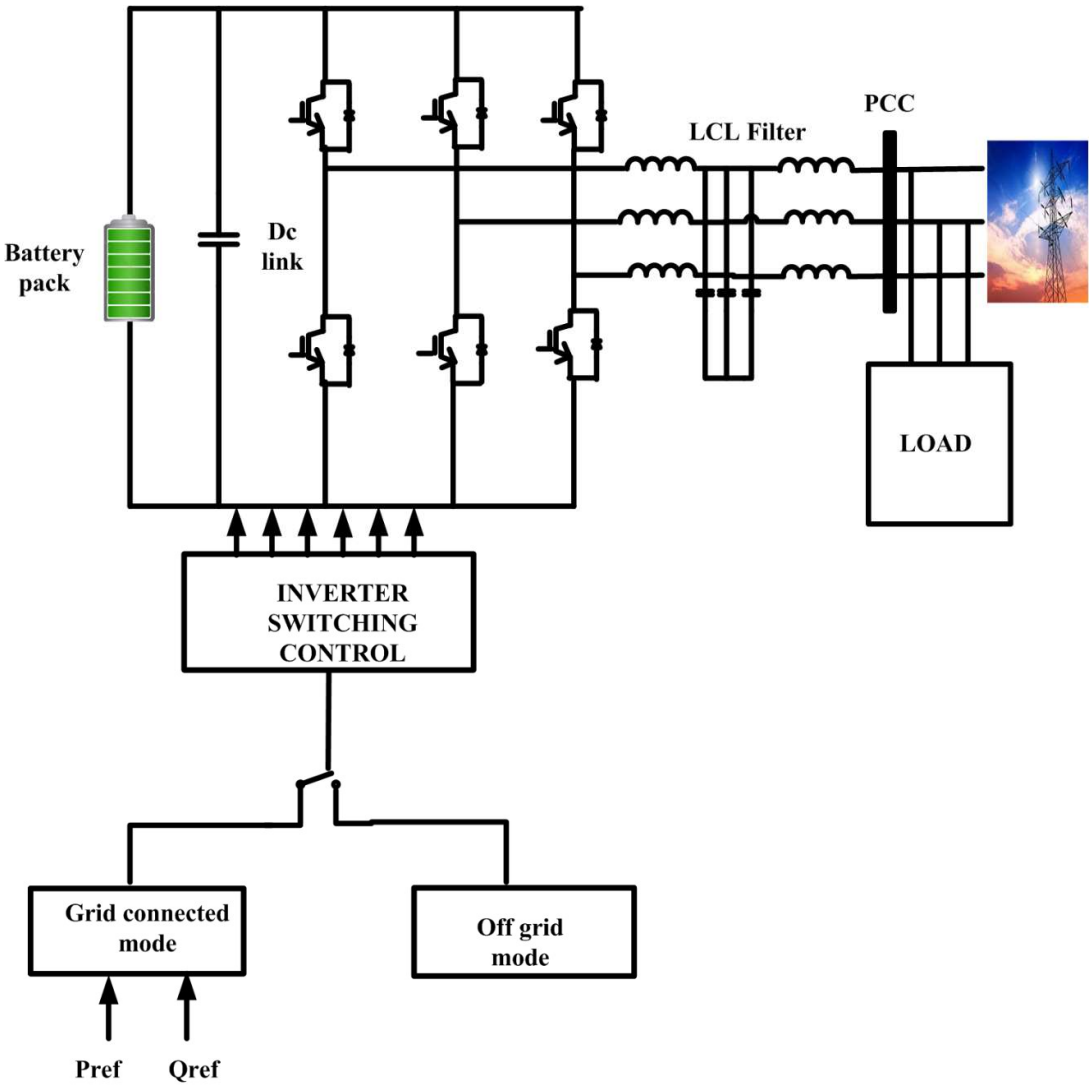

Figure 4.1: System description of VSC control in grid-connected and off-grid mode

The inverter is an essential component of solar photovoltaic and battery energy storage systems, and it plays a significant role in the renewable energy cycle. Grid-connected inverters, off-grid inverters, and On/Off Grid Tie Inverters are the three types of inverters. Each inverter has its own set of difficulties. The primary obstacles of using an off-grid inverter in a standalone system are to step up low DC battery voltage to AC supply voltage level in either single or three phase. Within its rated power capacity, it must be able to sustain the AC output voltage magnitude and frequency under varying load situations. The grid connected inverter, on the other hand, requires single or three phase synchronisation of phase, frequency, and magnitude with the utility grid. It is also necessary to regulate the delivery of actual and reactive power, as well as ride through capability during faults, in addition to grid synchronisation. When an islanding event occurs, it must also be able to detach from the grid. Finally, the On/Off Tie inverter can work in both islanded and grid tied micro grid circumstances.

Based on simplified converter model appropriate control strategy to show power flow management during both grid connected and off-grid mode is shown.

For simplicity of system, the simplified converter model of a three-phase voltage source converter (VSC) shown in Fig 4.1 is a two-level converter, which consists of a DC-Link, an inverter, and an LCL-filter connected to grid is connected to load at PCC. The inverter model consists of a self-commutated three-phase bridge, which is controlled by a pulse-width modulation signal.

The control structure includes two switches by which the operation mode, either grid-connected or off-grid mode, and therefore a corresponding converter control structure is selected. The objective is to achieve smooth transition between grid-connected and off-grid mode and to supply load during off-grid mode i.e. power flow management during transition between grid connected to off-grid mode. The transient voltage sag swell has to be investigated during transition.

4.3: Grid connected mode

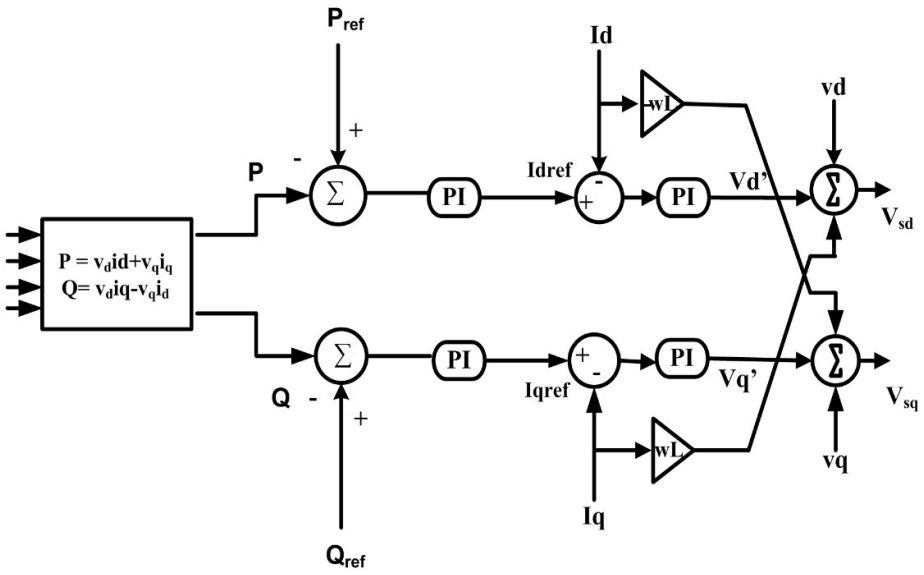

Figure 4.2: PQ control of VSC during grid connected mode

During grid-connected mode, the grid angle is given via a synchronous reference frame phase-locked loop (SRF-PLL)

Figure depicts the PQ controller's control principle. As illustrated in Figure, it has a PQ regulate loop and a current regulate loop. The measured inverter output voltages va, vb, vc, as well as currents ia, ib, ic, are translated to dq frames vd and vq, id and iq. The active P and reactive power Q of an inverter are computed as follows eqn (3.6) and eqn (3.7)

The inverter dq reference currents idref and iqref are obtained by a PI controller after being compared to their references Pref and Qref for load requirement:

$$id_{ref} = (kp_p + \frac{kp_i}{s})(P_{ref} - P) \quad (4.1)$$

$$iq_{ref} = (k_{pq} + \frac{k_{iq}}{s}) * (Q_{ref} - Q) \quad (4.2)$$

A PI controller regulates the inverter output currents id and iq by comparing them to the references idref and iqref. The outputs of the current regulators vsd and vsq are obtained after removing the interference of the coupling voltage and the output voltage vd, vq:

$$v_{sd} = \left(kp_p + \frac{kp_i}{s}\right)\left(id_{ref} - id\right) + wLi_q + v_d \quad (4.3)$$

$$v_{sq} = \left(k_{pq} + \frac{k_{iq}}{s}\right) * \left(iq_{ref} - iq\right) - wLi_d - v_q \quad (4.4)$$

4.4: Off-grid mode operation

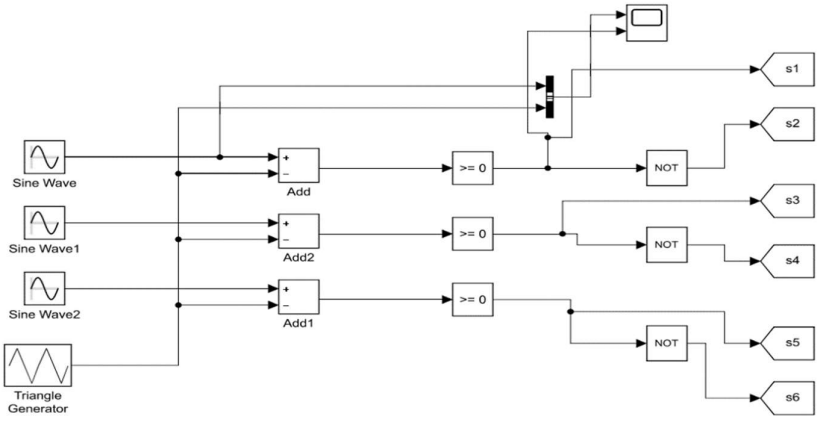

Figure 4.3: inverter switching during off-grid mode

During off-grid mode when grid is disconnected due to unplanned or planned islanding scenario the synchronisation of three phases voltage through grid is lost. Hence there is a difference in source and load power requirement. To mitigate voltage fluctuation and to supply load in such scenarios independent switching signals are provided to inverter, in this case load power requirement is fulfilled using battery energy storage system during off-grid mode as any islanding condition does not occur for longer duration hence storage system is designed which will be sufficient enough to supply load during this scenario.

For inverter switching the width of each pulse in Sinusoidal PWM is proportional to the amplitude of the sine wave evaluated at the centre of same pulse. As shown in Figure, the gating signals are created by comparing a sinusoidal reference wave with a triangle carrier wave of frequency Fr and Fc. Fr controls the Modulation Ratio (Ar/Ac) and hence the rms output voltage Vo, whereas Ar controls the inverter output frequency fo and its peak amplitude. The pulse width is a sinusoidal function of the angular position of the pulses in a cycle, and there are several pulses each half cycle. Here carrier wave frequency is chosen to be 10 kHz. A comparator compares a high frequency

carrier wave Vc to a reference signal Vr with the desired frequency. The output is high when the sinusoidal wave has a larger magnitude; otherwise, it is low. In a trigger pulse generator, the comparator output is processed so that the output voltage wave has a pulse width that matches the comparator pulse width.

4.5: Simulation result and discussion

The system model is simulated in MATLAB simulink software to validate performance of system working in both grid connected and offgrid mode.The main grid voltage is taken as 415 V rms and voltage level of battery pack is taken as 650 V dc.Three phase constant load is connected near PCC.In grid connected mode inverter control is done using PQ controller. During planned islanding circuit breaker switch disconnects the grid from the system, since there is mismatch between source and load requirement hence leads to voltage fluctuations. In offgrid mode load requirement is supplied by the battery pack with independent inverter switching.

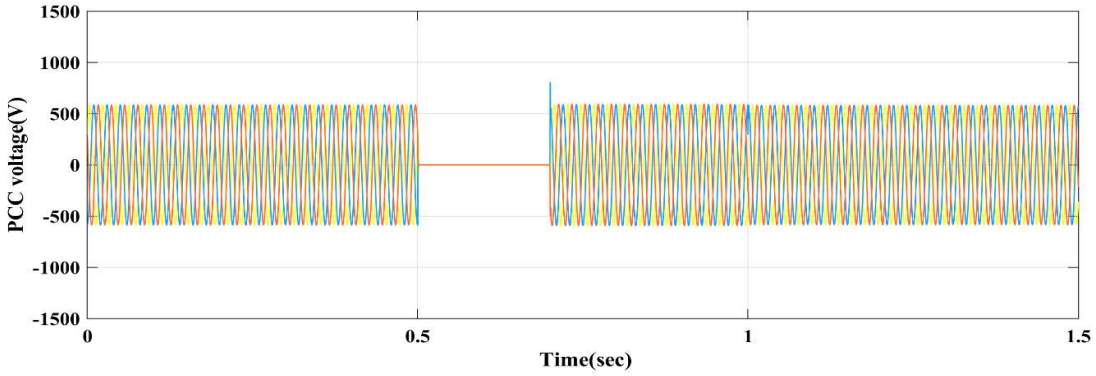

Figure 4.4 PCC voltage level

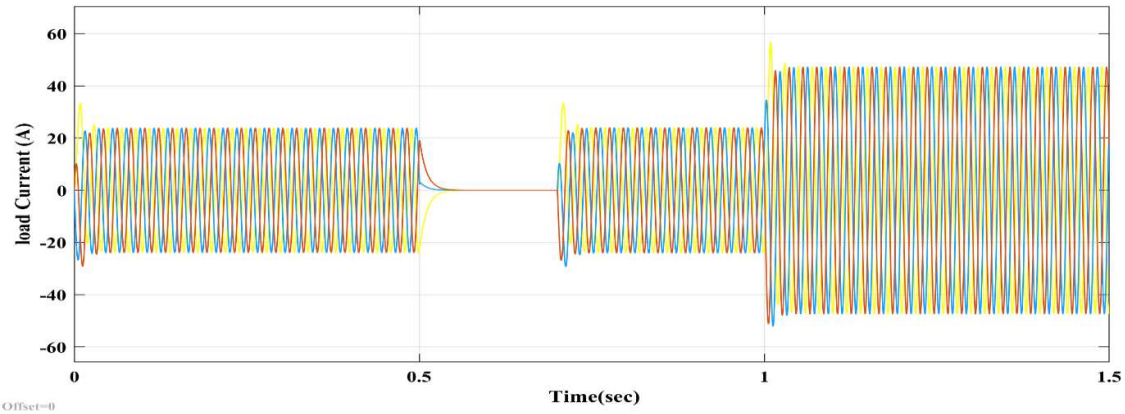

Figure 4.5: load current(A)

Fig. 4.4 shows PCC voltage level at different mode. The system is working in grid connected mode till t=0.5 sec with load of 10 kW, at 0.5 sec disconnection from grid leads to voltage fluctuation etc, at 0.7 sec control is switch to off grid inverter mode where battery storage system is fulfilling load requirement using independent SPWM inverter switching control.

Fig. 4.5 shows load current level showing three modes, first is the grid connected mode. Second is inverter working at off grid mode and third at t=1 sec where additional load of 10 kW is added to verify performance of system.

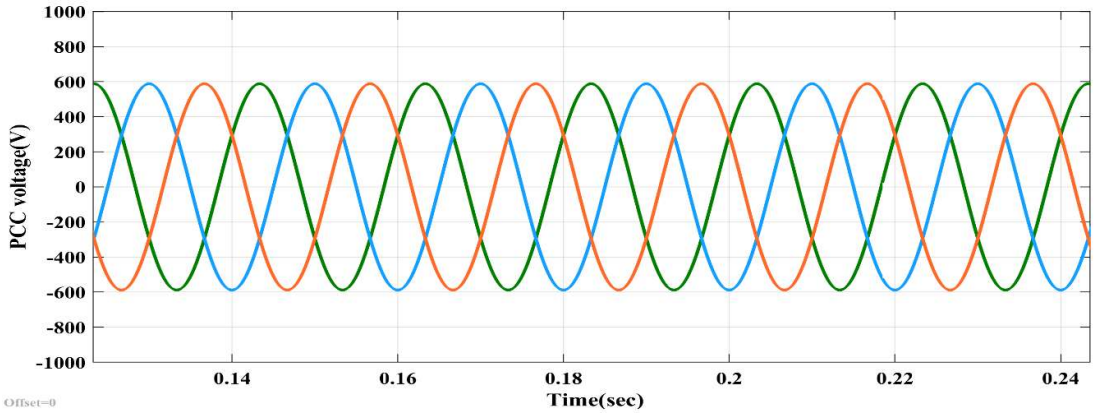

Figure 4.6 PCC voltage during grid connected mode

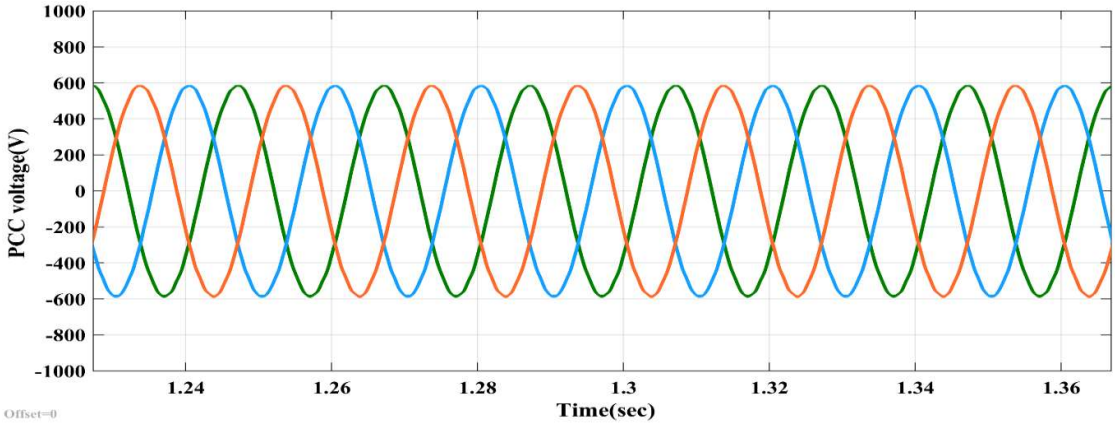

Figure 4.7: PCC voltage during off grid mode

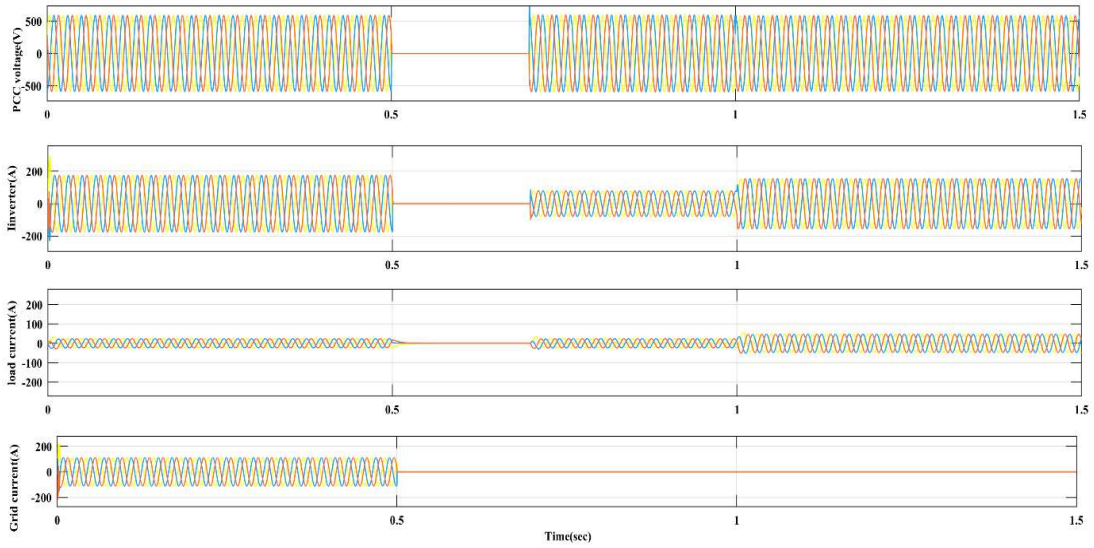

Figure 4.8: combined result of (a) PCC voltage (V) (b)inverter output current(A) (c) load current (A) (d) grid current(A)

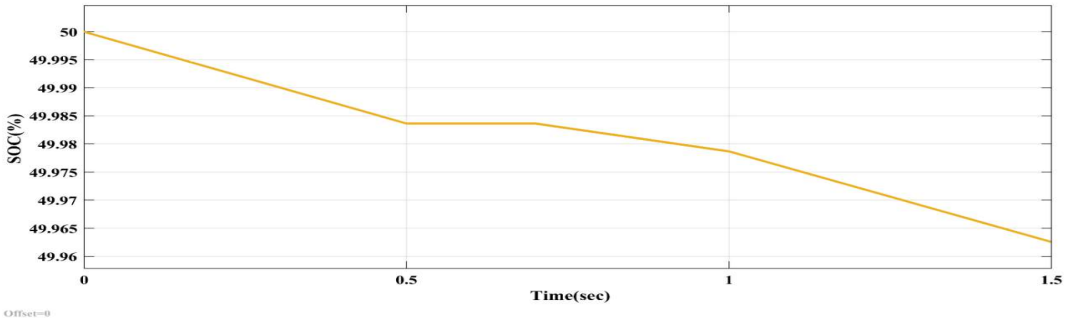

Figure 4.9: Battery SOC

Combined result of PCC voltage, inverter output current, load current and grid current is shown in Fig. 4.8. Battery SOC is shown in Fig. 4.9. for all modes. Load power level, inverter output power, grid power is shown in Fig. 4.10, 4.11, 4.12 respectively.

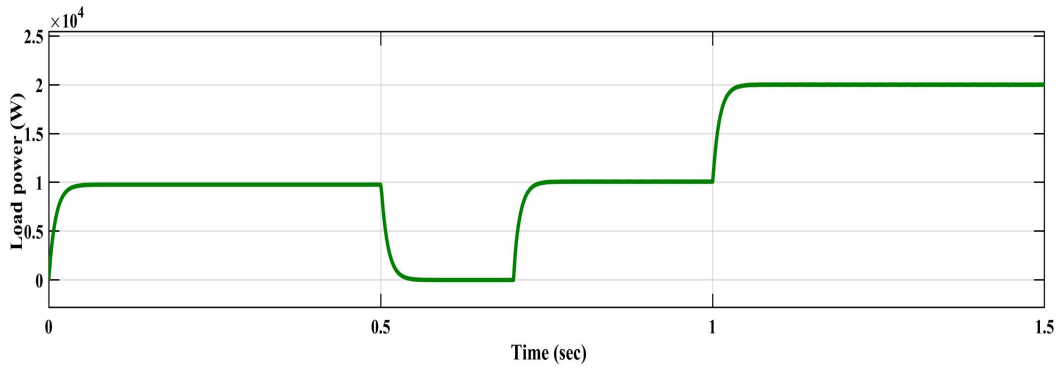

Figure 4.10: Load power (W)

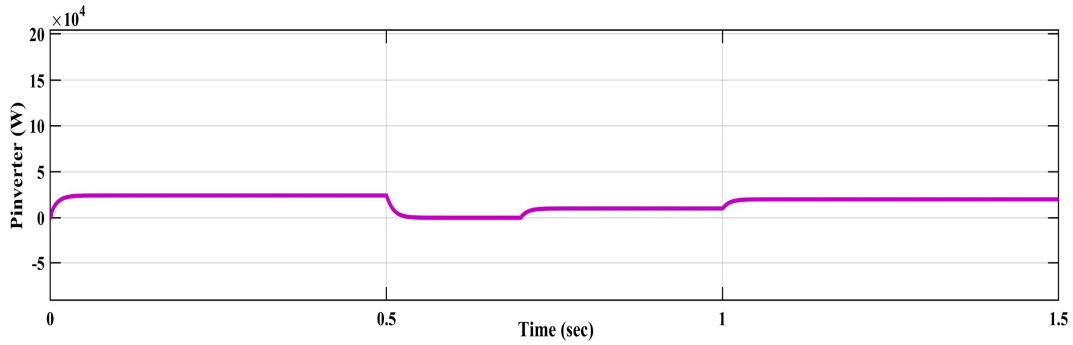

Figure 4.11: Inverter output power (W)

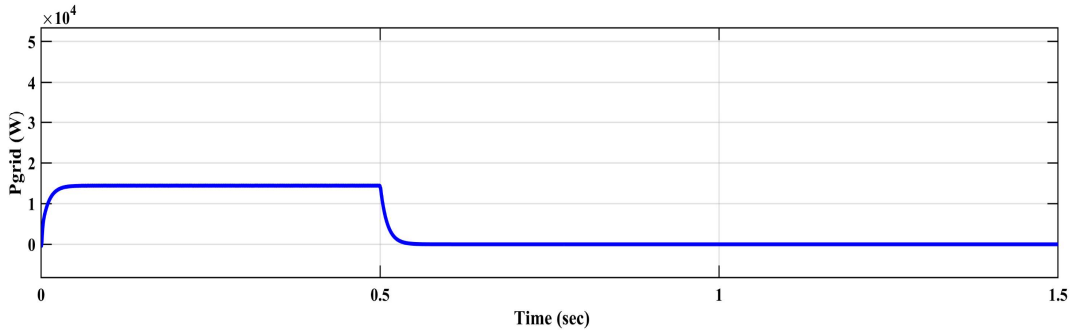

Figure 4.12: Grid power level (W)

CHAPTER 5

CONCLUSION AND FUTURE SCOPE

The main objective of work is detailed modelling and simulation of hybrid mode operation of Photovoltaic and Electric Vehicle charging system. The maximum power out of PV array is extracted with the help of DC-DC boost converter. In this work we are able to understand output the characteristics of photovoltaic array, designing of boost converter, designing of LCL filter. A controller at bi-directional DC-DC and an AC to DC stage are included in the associated controllers for EV charging/discharging and controlling various power flow modes. The EV charger can work in both modes of power flow i.e., grid to vehicle (G2V) and vehicle to grid (V2G), The system is modelled to charge or discharge EV based on PV power availability, EV charge state and grid requirement using bi-directional converters. Simple synchronous PI based controller are used in AC-DC control. To verify the performance of controller simulation for various modes have been carried out. This model is cost-effective and simple in design, and it supports PV power efficiency, continuous EV charging, and enhancement in grid power flow under a variety of load demand scenarios. Moreover, this model shows that the grid power quality will not be impacted in any of the power flow model.

Because large-scale renewable energy integration on the main grid can result in severe voltage fluctuations. As a result, BESS and on/off grid type inverters can be used as a backup to handle any fault and islanding situation. A small sub model showing power flow management to load during between transition to on-grid to off-grid operation is also shown. Grid power quality is also maintained in this case.

For future scope a hybrid model having solar photovoltaic system (PV), BESS, synchronous generator and electric vehicle charging system can be utilised to provide incessant charging during islanding, and grid connected mode using single VSC. Control strategy should include G2V power transfer for charging the EV and V2G power transfer for supporting the grid. A unified controller that can enables charging station to operate in both grid connected and islanding mode can be developed. Designing of an active power filter operation of the CS for mitigating the grid current harmonics can be done, so that the power exchange takes place at unity power factor. This is required for the compliance of the CS with the IEEE-519 standard.

List of Publication

- Mamta Gupta, A.K. Seth, M. Singh, “Grid Tied Photovoltaic Based Electric Vehicle Charging Infrastructure”, Second International Conference on Advances in Electrical, Computing, Communications and Sustainable Technologies, Bhilai, India 2022.

REFERENCES

[1] B. Pfluger and M. Wietschel, "Impact of renewable energies on conventional power generation technologies and infrastructures from a long-term least-cost perspective," *2012 9th International Conference on the European Energy Market*, 2012, pp. 1-10, doi: 10.1109/EEM.2012.6254768.

[2] S. K. Soonee *et al*., "Renewable Energy Integration in India: Present State and Long-Term Perspective," *2019 IEEE Milan PowerTech*, 2019, pp. 1-6, doi: 10.1109/PTC.2019.8810779.

[3] R. Arun, K. S. Mohammed Gohar Latheef, and G. Anandhakumar, "Grid interconnection of renewableenergy sources at the distribution level with powerquality improvement features," Int. J. Appl. Eng. Res., vol. 10, no. 33 Special Issue, pp. 25622–25626, 2015, doi: 10.23883/ijrter.conf.20171216.014.

[4] R. K. Rai, M. Dubey, M. Kirar and M. Kumar, "Analytical Analysis of Solar PV Module Using MATLAB," *2022 IEEE International Students' Conference on Electrical, Electronics and Computer Science (SCEECS)*, 2022, pp. 1-6, doi: 10.1109/SCEECS54111.2022.9741019.

[5] P. B. Joshi and S. R. Vaishnav, "A Simulation of Different Characteristics of Solar PV Grid Connected System," *2021 International Conference on Control, Automation, Power and Signal Processing (CAPS)*, 2021, pp. 1-5, doi: 10.1109/CAPS52117.2021.9730472.

[6] P. Shukl and B. Singh, "Hybrid Control of Solar PV-BES System Connected with 3P4W Utility Grid," *2021 IEEE 8th Uttar Pradesh Section International Conference on Electrical, Electronics and Computer Engineering (UPCON)*, 2021, pp. 1-6, doi: 10.1109/UPCON52273.2021.9667657.

[7] S. Afroze, R. Y. Udaykumar and A. Naik, "A systematic approach to grid connected PV system," *2012 IEEE Fifth Power India Conference*, 2012, pp. 1-5, doi: 10.1109/PowerI.2012.6479486.

[8] N. Karami, N. Moubayed, and R. Outbib, "General review and classification of different MPPT Techniques," Renew. Sustain. Energy Rev., vol. 68, no. September 2016, pp. 1–18, 2017, doi: 10.1016/j.rser.2016.09.132.

[9] N. Zinelaabidine, M. Karim, B. Bossoufi, and M. Taoussi, “MPPT algorithm control for grid connected PV module,” Proc. - 3rd Int. Conf. Adv. Technol. Signal Image Process. ATSIP 2017, pp. 1–6, 2017, doi: 10.1109/ATSIP.2017.8075527.

[10] C. Khomsi, M. Bouzid, and K. Jelassi, “Power quality improvement in a threephase grid tied photovoltaic system supplying unbalanced and nonlinear loads,” Int. J. Renew. Energy Res., vol. 8, no. 2, pp. 1165–1177, 2018.

[11] J. Saloman and T. S. Sirish, "Performance analysis of grid connected solar photo-voltaic system under grid abnormal conditions," *2016 International Conference on Signal Processing, Communication, Power and Embedded System (SCOPES)*, 2016, pp. 1653-1659, doi: 10.1109/SCOPES.2016.7955723.

[12] M. Fatima, A. S. Siddiqui and S. K. Sinha, "Grid integration of Renewable Sources in India: Issues and Possible Solutions," *2020 IEEE International Conference on Computing, Power and Communication Technologies (GUCON)*, 2020, pp. 506-510, doi: 10.1109/GUCON48875.2020.9231085..

[13] A. Narula and V. Verma, "Dual Port Impedance Converter for PV – Battery fed Remote Telecom Towers," 2018 IEEE 4th Southern Power Electronics Conference (SPEC), 2018, pp. 1-7, doi: 10.1109/SPEC.2018.8636089.

[14] H. Saxena, A. Singh and J. N. Rai, "Application of Time Delay Recurrent Neural Network for Shunt Active Power Filter in 3-Phase Grid-tied PV System," 2019 National Power Electronics Conference (NPEC), 2019, pp. 1-6, doi: 10.1109/NPEC47332.2019.9034769.

[15] M. O. Badawy and Y. Sozer, "Power Flow Management of a Grid Tied PV-Battery System for Electric Vehicles Charging," in IEEE Transactions on Industry Applications, vol. 53, no. 2, pp. 1347-1357, March-April 2017, doi: 10.1109/TIA.2016.2633526.

[16] C. Jain and B. Singh, "An Adjustable DC Link Voltage-Based Control of Multifunctional Grid Interfaced Solar PV System," in IEEE Journal of Emerging and Selected Topics in Power Electronics, vol. 5, no. 2, pp. 651-660, June 2017, doi: 10.1109/JESTPE.2016.2627533.

[17] A. Verma, B. Singh, A. Chandra and K. Al-Haddad, "An Implementation of Solar PV Array Based Multifunctional EV Charger," 2018 IEEE Transportation Electrification Conference and Expo (ITEC), 2018, pp. 531-536, doi: 10.1109/ITEC.2018.8450191

[18] Un-Noor, F., Sanjeev Kumar P., Mihet-popa, L., Mollah, M.N., Hossain, E, "A comprehensive study of key electric vehicle (EV) components, technologies, challenges, impacts, and fiture direction of development," Energies, vol. 10, p. 1217, 2017

[19] G. Soares dos Santos, F. José Grandinetti, R. Augusto Rocha Alves and W. de Queiróz Lamas, "Design and Simulation of an Energy Storage System with Batteries Lead Acid and Lithium-Ion for an Electric Vehicle: Battery vs. Conduction Cycle Efficiency Analysis," IEEE Latin America Transactions, vol. 18, no. 8, pp. 1345-1352, 2020.

[20] A. Emadi, Y. J. Lee and K. Rajashekara, "Power Electronics and Motor Drives in Electric, Hybrid Electric, and Plug-In Hybrid Electric Vehicles," IEEE Transactions on Industrial Electronics, vol. 55, no. 6, pp. 2237-2245, 2008.

[21] F. U. Syed, M. L. Kuang and H. Ying, "Active Damping Wheel-Torque Control System to Reduce Driveline Oscillations in a Power-Split Hybrid Electric Vehicle," IEEE Transactions on Vehicular Technology, vol. 58, no. 9, pp. 4769- 4785, 2009.

[22] S. Shafiee, M. Fotuhi-Firuzabad and M. Rastegar, "Impacts of controlled and uncontrolled PHEV charging on distribution systems," in 9th IET International Conference on Advances in Power System Control, Operation and Management (APSCOM 2012), 2012.

[23] R. Jurgen, "Fuel-Cell hybrid EVs," Electric and hybrid electric vehicles, p. 9, 2011.

[24]. Z. Huang, S. Wong and C. K. Tse, "An Inductive-Power-Transfer Converter With High Efficiency Throughout Battery-Charging Process," IEEE Transactions on Power Electronics, vol. 34, no. 10, pp. 10245-10255, 2019.

[25] S.S. Williamson and B. Peschiera , "Review and comparison of inductive charging power electronic converter topologies for electric and plug-in hybrid electric vehicles," in IEEE Transportation Electrification Conference and Expo (ITEC), Detroit, MI, 2013.

[26] M. Forouzesh, Y. P. Siwakoti, S. A. Gorji, F. Blaabjerg and B. Lehman, "StepUp DC DC Converters: A Comprehensive Review of Voltage-Boosting Techniques, Topologies, and Applications," IEEE Transactions on Power Electronics, vol. 32, no. 12, pp. 9143-9178, 2017.

[27] Murat Yilmaz, and Philip T. Krein, “Review of Battery Charger Topologies, Charging Power Levels, and Infrastructure for Plug-In Electric and Hybrid Vehicles”, IEEE transactions on power elec., vol. 28, no. 5.

[28] M. A. Hannan, M. M. Hoque, S. E. Peng and M. N. Uddin, "Lithium-Ion Battery Charge Equalization Algorithm for Electric Vehicle Applications," IEEE Transactions on Industry Applications, vol. 53, no. 3, pp. 2541-2549, 2017.

[29] S. R. Ovshinsky et al., "Advanced materials for next generation NiMH portable, HEV and EV batteries," IEEE Aerospace and Electronic Systems Magazine, vol. 14, no. 5, pp. 17-23, 1999.

[30] X. Wei, X. Zhao and Y. Yuan, "Study of Equivalent Circuit Model for Lead-Acid Batteries in Electric Vehicle," in International Conference on Measuring Technology and Mechatronics Automation, Zhangjiajie, Hunan, 2009.

[31] L. Cheng, Y. Chang and R. Huang, “Mitigating Voltage Problem in Distribution System With Distributed Solar Generation Using Electric Vehicles,” IEEE Trans. Sustainable Energy, vol. 6, no. 4, pp. 1475- 1484, Oct. 2015, doi: 10.1109/TSTE.2015.2444390.

[32] M. Brenna, F. Foiadelli and M. Longo, “The Exploitation of Vehicleto Grid Function for Power Quality Improvement in a Smart Grid,” IEEE Trans. Intelligent Transportation Systems, vol. 15, no. 5, pp. 2169-2177, Oct. 2014, doi: 10.1109/TITS.2014.2312206.

[33] N. Saxena, I. Hussain, B. Singh and A. L. Vyas, "Implementation of a Grid-Integrated PV-Battery System for Residential and Electrical Vehicle Applications," in IEEE Transactions on Industrial Electronics, vol. 65, no. 8, pp. 6592-6601, Aug. 2018, doi: 10.1109/TIE.2017.2739712.

[34] L. Wang, Z. Qin, T. Slangen, P. Bauer and T. van Wijk, "Grid Impact of Electric Vehicle Fast Charging Stations: Trends, Standards, Issues and Mitigation Measures - An Overview," in IEEE Open Journal of Power Electronics, vol. 2, pp. 56-74, 2021, doi: 10.1109/OJPEL.2021.3054601.

[35] A. Verma and B. Singh, "Control and Implementation of Renewable Energy Based Smart Charging Station Beneficial for EVs, Home and Grid," 2019 IEEE Energy Conversion Congress and ExpositionECCE), 2019, pp. 5443-5449, doi: 10.1109/ECCE.2019.8913253.

[36] B. Singh, A. Verma, A. Chandra, and K. Al-Haddad, "Implementation of Solar PV-Battery and Diesel Generator Based Electric Vehicle Charging Station," IEEE Transactions on Industry Applications, vol. 56, no. 4, pp. 4007-4016, 2020, doi: 10.1109/TIA.2020.2989680.

[37] K. Chaudhari, A. Ukil, K. N. Kumar, U. Manandhar, and S. K. Kollimalla, “Hybrid optimization for economic deployment of ESS in PV-integrated EV charging stations,” IEEE Trans. Ind. Inform., vol. 14, no. 1, pp. 106– 116, Jan. 2018.

[38] F. Kineavy and M. Duffy, “Modelling and design of electric vehicle charging systems that include on-site renewable energy sources,” in Proc. IEEE 5th Int. Symp. Power Electron. Distrib. Gene r. Syst., 2014, pp. 1–8.

[39] Y. Zhang, P. You, and L. Cai, “Optimal charging scheduling by pricing for EV charging station with dual charging modes,” IEEE Trans. Intell. Transp. Syst., vol. 20, no. 9, pp. 3386–3396, Sep. 2019.

[40] Y. Yang, Q. Jia, G. Deconinck, X. Guan, Z. Qiu, and Z. Hu, “Distributed coordination of EV charging with renewable energy in a microgrid of buildings,” IEEE Trans. Smart Grid, vol. 9, no. 6, pp. 6253–6264, Nov. 2018.

[41] N. K. Kandasamy, K. Kandasamy, and K. J. Tseng, “Loss-of-life investigation of EV batteries used as smart energy storage for commercial building-based solar photovoltaic systems,” IET Elect. Syst. Transp., vol. 7, no. 3, pp. 223–229, 2017.

[42] H. Laaksonen, P. Saari, and R. Komulainen, “Voltage and frequency control of inverter based weak LV network microgrid,” presented at the Int. Conf. Future Power Syst., Amsterdam, The Netherlands, Nov. 18, 2005.

[43] S. Adhikari and F. Li, "Coordinated V-f and P-Q Control of Solar Photovoltaic Generators With MPPT and Battery Storage in Microgrids," in *IEEE Transactions on Smart Grid*, vol. 5, no. 3, pp. 1270-1281, May 2014, doi: 10.1109/TSG.2014.2301157.

[44] P. Zhongmei, H. Tonghui and W. Yuqing, "Voltage sags/swells subsequent to islanding transition of PV-battery microgrids," *2016 IEEE 11th Conference on Industrial Electronics and Applications (ICIEA)*, 2016, pp. 2317-2321, doi: 10.1109/ICIEA.2016.7603978.

[45].Nayak, Pravati, et al. "Optimal PQ Control of Solar Photovoltaic Based Microgrids with Battery storage." 2019 Innovations in Power and Advanced Computing Technologies (i-PACT). Vol. 1. IEEE, 2019.

[46] N. Hajilu, G. B. Gharehpetian, S. H. Hosseinian, M. R. Poursistani and M. Kohansal, "Power control strategy in islanded microgrids based on VF and PQ theory using droop control

of inverters," *2015 International Congress on Electric Industry Automation (ICEIA 2015)*, 2015, pp. 37-42, doi: 10.1109/ICEIA.2015.7165844.